Yeager Airport RSS Failure Case History: Forensic Limit Equilibrium and FLAC Analyses

Jim Collin, Ph.D., P.E., D.GE., F. ASCE
The Collin Group, Ltd.
jim@thecollingroup.com

Timothy D. Stark, Ph.D., P.E., D.GE., F. ASCE
University of Illinois at Urbana-Champaign
tstark@illinois.edu

Augusto Lucarelli
Itasca Consulting Group
alucarelli@itascacg.com

Yeager Airport RSS Failure Case History

Ryan Berg, P.E., D.GE., F. ASCE
Ryan R Berg & Associates
ryanberg@att.net

Jim Collin, Ph.D., P.E., D.GE., F. ASCE
The Collin Group, Ltd.
jim@thecollingroup.com

Related Technical Papers

Check for updates

ASCE

Stability and Stress-Deformation Analyses of Reinforced Slope Failure at Yeager Airport

James G. Collin, Ph.D., P.E., D.GE, F.ASCE[1]; Timothy D. Stark, Ph.D., P.E., D.GE, F.ASCE[2]; Augusto Lucarelli, M.ASCE[3]; Thomas P. Taylor, Ph.D., P.E., D.GE, F.ASCE[4]; and Ryan R. Berg, P.E., D.GE, F.ASCE[5]

Abstract: This paper describes the material properties along with the inverse limit-equilibrium and permanent deformation analyses used to investigate the 2015 reinforced slope failure at the Yeager Airport near Charleston, West Virginia. Inverse two-dimensional (2D) limit-equilibrium analyses were first performed to evaluate laboratory-derived strength parameters, slope geometry, and soil reinforcement configuration that would reproduce the observed critical failure surface. Because of the shape of the reinforced soil slope (RSS) (outside radius), the impact of the direction of the uniaxial geogrid reinforcement, varying from parallel to almost perpendicular to the direction of sliding, was analyzed using a three-dimensional (3D) limit-equilibrium analysis. Finite-difference permanent deformation analyses were also conducted to understand the internal stresses and deformations of the RSS prior to failure and kinematics of the slope failure. The results of these various analyses are consistent with postfailure field observations and demonstrate the value of performing multiple types of analyses, e.g., 2D and 3D limit-equilibrium and permanent deformation analyses, when analyzing a complex slope failure. **DOI: 10.1061/(ASCE)GT.1943-5606.0002454.** *© 2020 American Society of Civil Engineers.*

Author keywords: Geogrids; Inverse analysis; Shear strength; Anisotropy; Slope stability; Compacted fill; Fully softened strength; Residual strength; Strength-reduction method; Numerical analysis.

Introduction

Yeager Airport near Charleston, West Virginia, was constructed atop mountainous terrain in 1947. Construction of the airport involved excavating several hilltops and filling the adjacent valleys to create a nearly horizontal plateau for the runways, taxiways, roads, and accompanying infrastructure. The earthwork required 3 years to complete and at the time was the second largest earth-moving project in history, but well behind the Panama Canal (Lostumbo 2010). The earthwork involved moving more than 6.88 million m^3 (9 million cu yd) of earth and rock and required more than 910,000 kg (2 million lb) of explosives to facilitate rock excavation (Lostumbo 2010). Because the airport was constructed on hilltop ridges, the ground surface slopes steeply down to the surrounding Elk and Kanawha River Valleys.

To comply with new airport regulations, Yeager Airport was required to extend Runway 5 by 150 m (500 ft) to create a longer emergency stopping area. This was quite a challenge because the runway extension would be over a 91-m (300-ft)-high steep slope. A reinforced steepened slope was selected to extend the runway instead of other options because it offered an economical solution that was believed to be easy to construct and blend in with the surrounding green hills of West Virginia (Lostumbo 2010). This resulted in the tallest [72 m (240 ft)] $1H{:}1V$ (45°) geosynthetic reinforced vegetated slope known in the United States in 2007 when it was completed (Lostumbo 2010). Unfortunately, the slope failed in 2015, 8 years after construction.

The reinforced soil slope (RSS) was constructed with a primary and secondary zone of geogrid reinforcement. The primary reinforcement, strips of polyester uniaxial geogrids, was used to construct the majority of the RSS. Two types of uniaxial geogrids were used in the primary reinforcement zone, namely 10G and 20G geogrids with long-term allowable tensile strengths, i.e., ultimate strengths reduced for installation damage, of 49.6 kN/m (3,400 lb/ft) and 66.1 or 145.9 kN/m (4,530 lb/ft), respectively.

Fig. 1(a) shows a layer of the black primary geogrid being placed below the slope crest. Fig. 1(a) also shows the secondary reinforcement zone, which was used to support the face of the RSS and consisted of a lightweight geogrid face wrap. This lightweight geogrid consists of a small-aperture mesh-type geogrid comprised of a green woven polypropylene mesh that provided erosion protection and allowed for fast germination of the vegetation on the slope face (Lostumbo 2010).

The constructed reinforced slope started to show movement about 2 years prior to failure, with cracks first appearing in the crest of the slope along the back of the RSS mass in 2013, or 6 years after completion. By February 2014, large deformations and tension cracks were visible in the slope crest and runway. The slope failed on March 12, 2015 (Fig. 1), after 8 years of service. This paper

[1]President, Collin Group, 7445 Arlington Rd., Bethesda, MD 20184. Email: jim@thecollingroup.com

[2]Professor, Dept. of Civil and Environmental Engineering, Univ. of Illinois at Urbana-Champaign, 205 N. Mathews Ave., Urbana, IL 61801 (corresponding author). ORCID: https://orcid.org/0000-0003-2384-1868. Email: tstark@Illinois.edu

[3]Principal, Itasca Consulting Group, Inc., 111 3rd Ave. South, Suite 450, Minneapolis, MN 55401. Email: alucarelli@itascacg.com

[4]Civil Engineering Consultant, Ground Improvement Systems, LLC 2301 Poplar LN Colleyville, TX 76034. ORCID: https://orcid.org/0000-0001-7828-2894. Email: tptaylor.pe@gmail.com

[5]President, Ryan R Berg & Associates, 2190 Leyland Alcove, Woodbury, MN 55125-3504. ORCID: https://orcid.org/0000-0002-7013-0711. Email: ryanberg@att.net

Note. This manuscript was submitted on April 1, 2020; approved on September 15, 2020; published online on December 28, 2020. Discussion period open until May 28, 2021; separate discussions must be submitted for individual papers. This paper is part of the ***Journal of Geotechnical and Geoenvironmental Engineering***, © ASCE, ISSN 1090-0241.

Stark et al. (2021) ©

ARTICLE IN PRESS

Geotextiles and Geomembranes xxx (xxxx) xxx

Contents lists available at ScienceDirect

Geotextiles and Geomembranes

journal homepage: www.elsevier.com/locate/geotexmem

ELSEVIER

Professional Practice Paper

Case history on failure of a 67 M tall reinforced soil slope

Ryan R. Berg[a,*], James G. Collin[b], Thomas P. Taylor[c], Chester F. Watts[d]

[a] *Ryan R Berg & Associates, 2190 Leyland Alcove, Woodbury, MN, 55125-3504, USA*
[b] *The Collin Group, 7445 Arlington Road, Bethesda, MD, 20184, USA*
[c] *Ground Improvement Systems, LLC, 114 South Collins Street, Arlington, TX, 76011, USA*
[d] *Director of Geohazards & Unmanned Systems Research Center, Reed Hall, Box 6939, Radford University, Radford, VA, 24142, USA*

ARTICLE INFO

Keywords:
Reinforced soil slope
Geogrid
Failure
Compound failure plane
Case history

ABSTRACT

Construction of this 67 m high *RSS* was completed in December 2006. After seven years in-service, a tension crack was observed at the top of the slope. In March 2015 this *RSS* structure catastrophically collapsed. This *RSS* structure collapsed in a compound failure mode; as the failure plane passed beneath, partially behind, and partially through the reinforced soil mass. The failure plane beneath the *RSS* was along a shale-claystone interface. The failure surface partially behind the *RSS* was along sandstone bedrock with water-seeping bedding planes dipping out of the rock mass. The failure surface through the upper portion of the *RSS* is where the geogrid reinforcement was overwhelmed by stresses originating from underlying deformation. The *RSS* collapse occurred after 8.3 years in-service as the shear strength along the shale-claystone interface decreased and approached the fully softened strength. The primary causative factors of this failure are: (i) an insufficient subsurface investigation program and interpretation of data for design and detailing; (ii) insufficient specifications and construction plan details for both foundation preparation and rock backcut benching; (iii) insufficient foundation preparation and rock backcut benching during construction; and (iv) adaptations to the design made during construction.

1. Introduction

Construction of the tallest reinforced soil slope (*RSS*) in the United States was completed in December 2006, at Yeager Airport, located near Charleston, West Virginia. This 67 m (*m*) high *RSS* structure was designed and constructed as part of the airport's 2005 facility upgrades. The purpose of the *RSS* was to support a 152 *m* extension of Runway 5; on which an engineered mass arresting system for emergency stops was installed. This *RSS* structure catastrophically failed on 12 March 2015; fortunately without loss of life, but it did result in extensive property loss and damage.

This project, the failure of the structure, and this forensic analysis work is unique in several aspects. The *RSS* structure is unique due to its height and the massive amount of geogrid soil reinforcement within it. The structure was in-service for many years and had been performing well. Movements started being observed about two years prior to failure. Therefore something changed, either the resistance decreased or the loading increased, or a combination of the two. The *RSS* suffered a catastrophic collapse, which is infrequent in *RSS* failures. The failure plane passed through approximately 30 *m* of the reinforced soil, and by visual observation, was in internal or compound (Berg et al., 1989) failure mode. Such is rarely seen in *RSS* failures, and certainly none of this magnitude. The failure plane was well defined and therefore could be used in back analyses. Additionally, the structure was convex in plan view, and there were three dimensional (*3D*) aspects to construction, failure, and stability analyses to be considered. To the best of our knowledge, *3D* analysis of a convex, uniaxial geogrid reinforced soil slope had not been attempted prior to this work. Again, *3D* analyses are rarely seen in *RSS* structures and this is the first with a documented failure.

The authors of this case history were members of one of the several engineering teams investigating this failure. Our team worked for the owner's insurance company and then for attorneys representing the owner, Central West Virginia Regional Airport Authority (*CWVRAA*), in litigation. This paper is based upon: (i) our review of design and construction records; (ii) observations during removal of the remaining *RSS* fill and excavation of investigatory trenches; (iii) laboratory testing of soils and geogrids used in construction; (iv) subsequent subsurface investigation (by others) for repair works; and (v) our analyses (Collin et al., 2018). Additionally, some insights were gained from

* Corresponding author.
E-mail addresses: ryanberg@att.net (R.R. Berg), jim@thecollingroup.com (J.G. Collin), tptaylor.pe@gmail.com (T.P. Taylor), cwatts@radford.edu (C.F. Watts).

https://doi.org/10.1016/j.geotexmem.2020.06.003
Received 27 March 2020; Received in revised form 15 June 2020; Accepted 22 June 2020

Please cite this article as: Ryan R. Berg, *Geotextiles and Geomembranes*, https://doi.org/10.1016/j.geotexmem.2020.06.003

Today's Webinar

- Forensic investigation involved an extensive field exploration, laboratory testing, and detailed engineering analyses – the entire process took over two years.
- Purpose – Share details of forensic 2D and 3D limit equilibrium and Continuum Deformation analyses
- Our client was the West Virginia Regional Airport Authority

Outline

- 12 March 2015 Failure - Collin
- Laboratory Testing – Collin and Stark
- 2D Limit Equilibrium Analyses - Stark
- 3D Limit Equilibrium Analyses – Stark
- Continuum Deformation Analyses - Lucarelli
- Summary - Collin

Timeline

- August 2005 - RSS Construction started
- December 2006 - RSS Construction Completed
- 2010 through 2014 - Shallow slides at base of RSS
- July 2013 - First cracks in EMAS noted
- January 2015 – Settlement of EMAS observed
- March 12, 2015 - Catastrophic failure

RSS Construction Completed

Stark et al. (2021) ©

Failure March 2015

Stark et al. (2021) ©

Failure Closed Keystone Drive Below RSS

Stark et al. (2021) ©

Failure March 2015

Stark et al. (2021) ©

Original Design

- 250 ft/76.3 m high slope
- 175 ft/53.4 m long geogrid
- 1H:1V

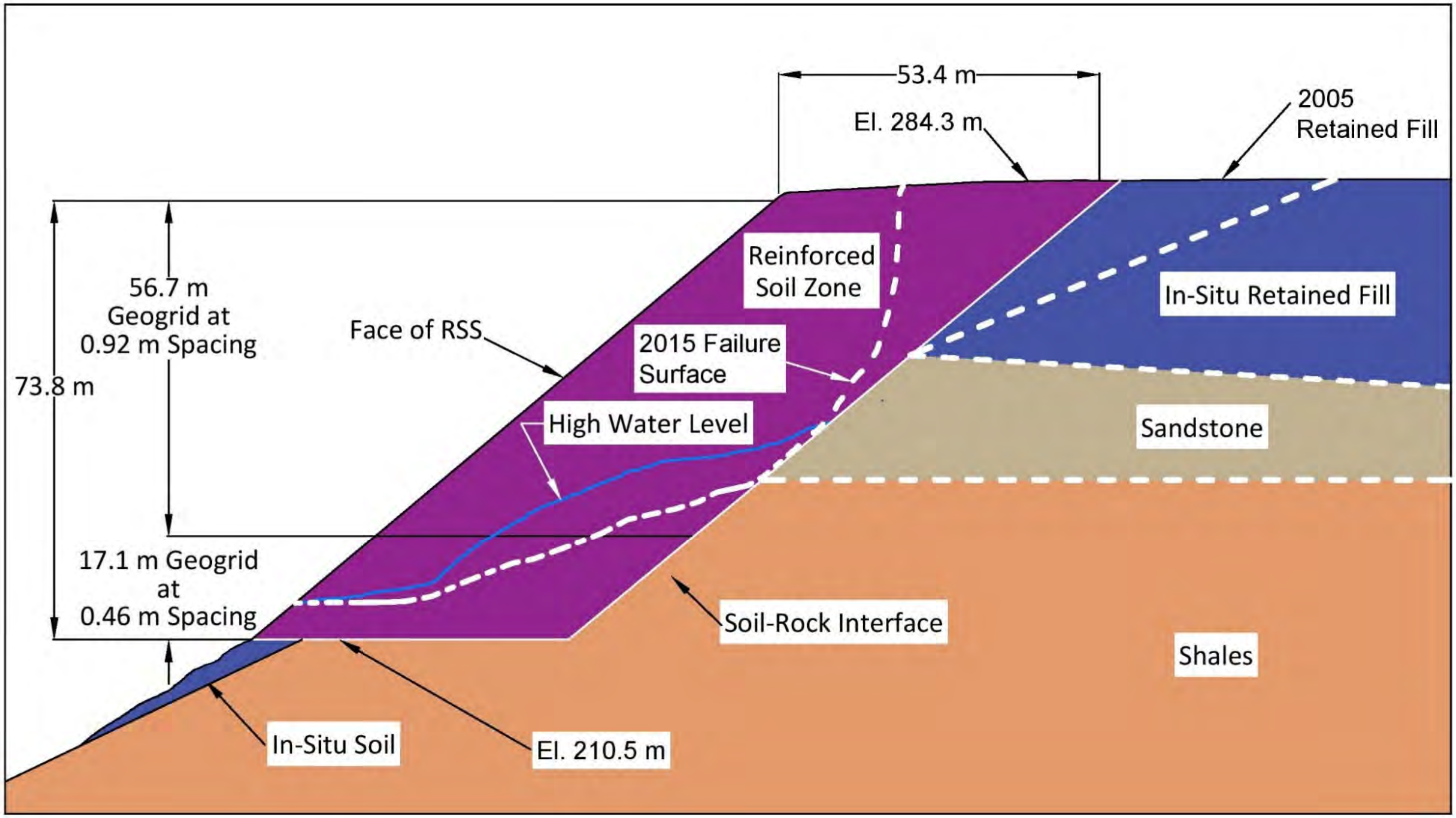

Stark et al. (2021) ©

Forensic Cross-Section

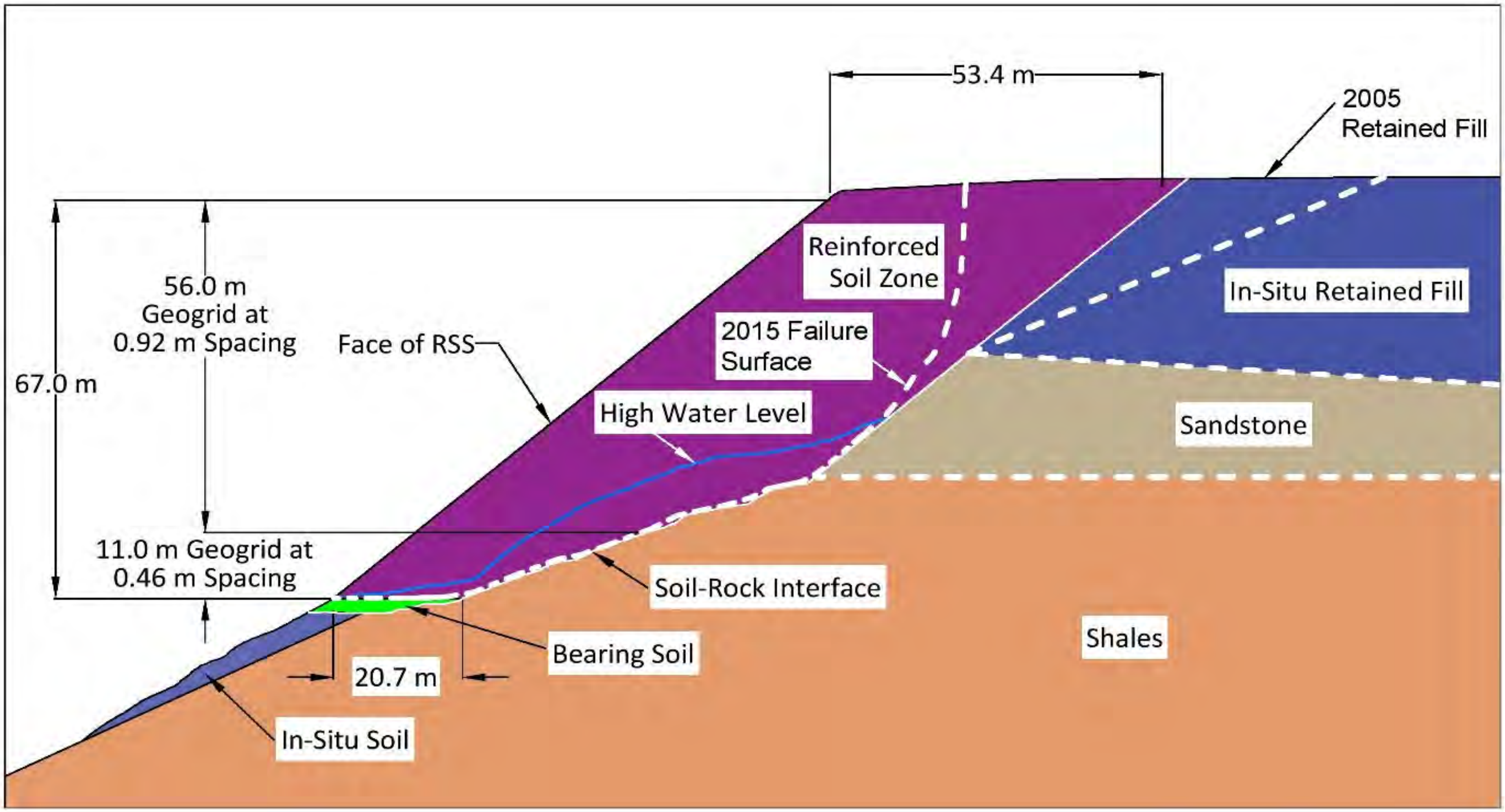

Stark et al. (2021) ©

Failure Mechanism

- Compound failure mode
- Failure surface below RSS was along a shale-claystone interface
- RSS collapse occurred after 8 years in-service as shear strength of shale-claystone interface decreased from peak towards the fully softened strength

Outline

- 12 March 2015 Failure
- Laboratory Testing – Stark
- 2D Limit Equilibrium Analyses
- 3D Limit Equilibrium Analyses
- Continuum Deformation Analyses
- Summary

Original Design

Geogrid Material Properties							
Geogrid	T_{ult} (plf)	RF_{CR}	RF_{CR}	RF_{D}	RF_{ID}	RF_{ID}	T_a (plf)
A	9,950	1.67	1.9	1.15	1.11	1.3	3,502
B	12,870	1.72	1.9	1.15	1.05	1.3	4,530

Exhumed Geogrid

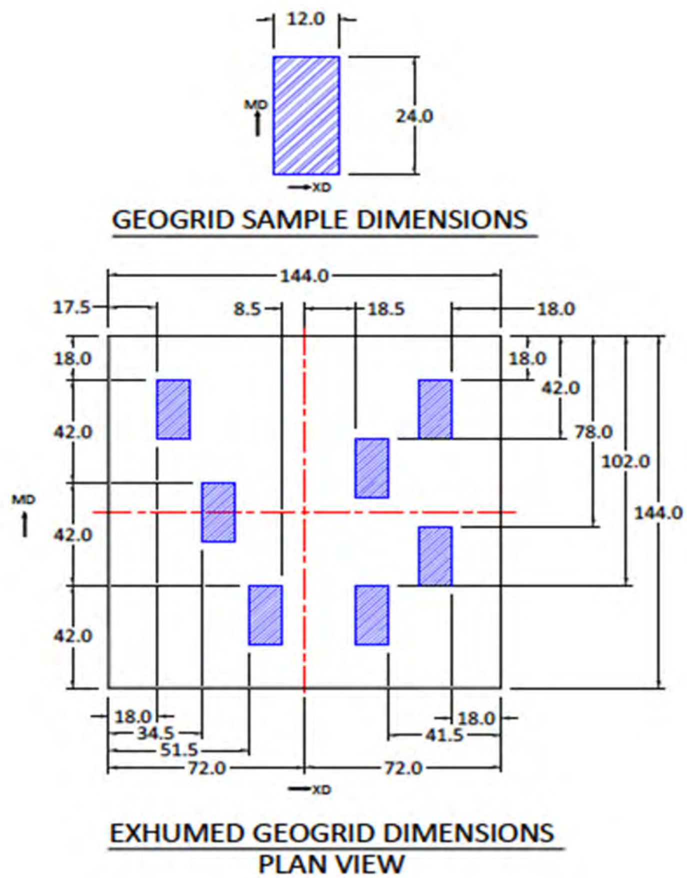

Exhumed Geogrid Testing Results

Exhumed Geogrid Wide Width and Single Rib Test Results			
Geogrid Type	Wide Width strength (lbs/ft)	Single Rib Strength (lbs/ft)	Strength Used in Analysis (lbs/ft)
A	7,511	9,165	9,000
B	9,037	9,848	10,000

Failure Surface Identified

Soil/Rock Interface

- **LL = 32 – 40**
- **PI = 11 - 19**
- **CF = 45 - 46**

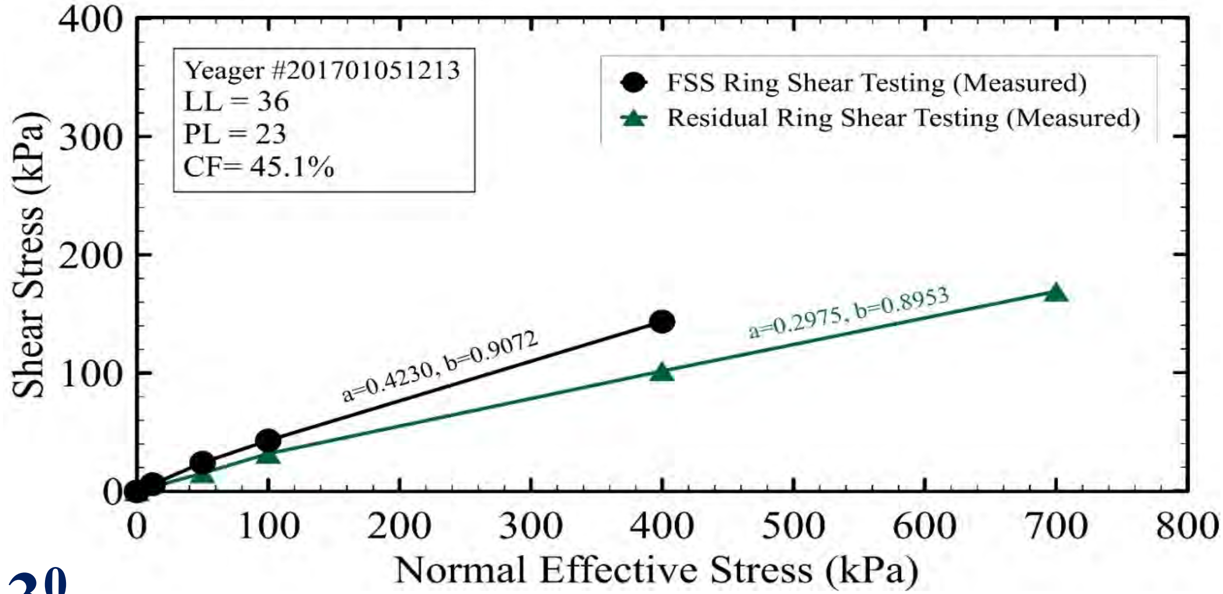

- **FSS = 27 – 21^0**
- **Residual = 18 – 13^0**

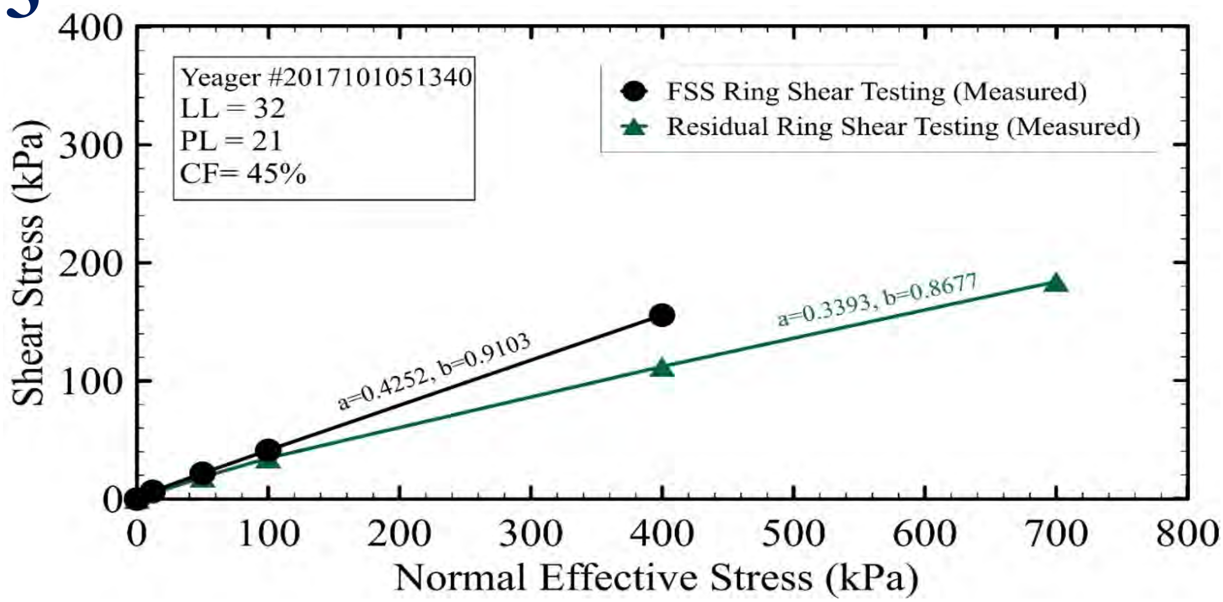

Soil/Rock Interface

- **FSS = 26 – 20^0**
- **Residual = 17 - 14^0**
- **Correlations – Stark and Eid (1997)**

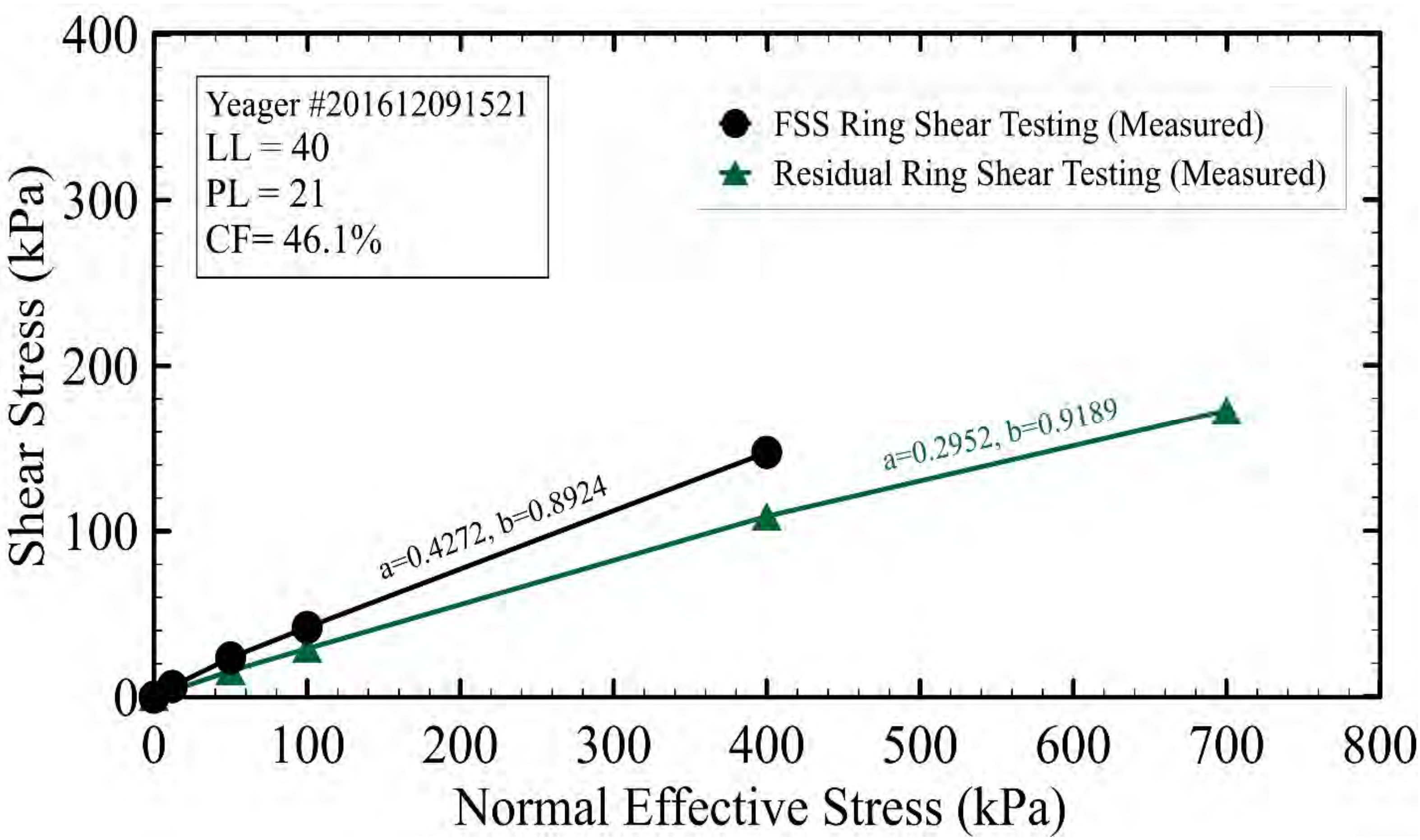

Soil Properties

Slope Material	Moist Unit Weight γ_{moist} (pcf/kN/m^3)	Effective Stress Friction Angle ϕ' (deg)	Effective Stress Cohesion c' (psf/kPa)
Reinforced Soil Zone	135/21.2	36^o	0
In-Situ Retained Soil Zone	135/21.2	36^o	0
Bearing Soil at Slope Toe	135/21.2	36^o	0
Soil/Rock Interface	135/21.2	Stress-dependent strength envelope	0

Outline

- 12 March 2015 Failure
- Laboratory Testing
- 2D Limit Equilibrium Analyses
- 3D Limit Equilibrium Analyses
- Continuum Deformation Analyses
- Summary

2D Stability Analyses

Design Cases			
Case	Name	Scenario	Notes
1	Initial Design – Rock	L1+G1+S1+Drained	Geogrid Long-Term Design Strength (LTDS=66.1 kN/m), Uniform,175 ft, & 36^0
2	Revised Design - Rock	L2+G1+S1+Drained	Geogrid LTDS, 80-175 ft, & 36^0
3	End of Construction (Short-Term)	L2+G2+S2+Drained	Exhumed geogrid strength (145.9 kN/m), Variable geogrid length, & 36^0

$$G1 = LTDS = RF_{ID} + RF_{Degradation} + RF_{CR}$$

2D Stability Results

2D Factors of Safety for Cases 1-3 Fully Drained		
Design Case	Water Condition	2D FS
1. Initial Design (LTDS & Rock)	Dry	1.54
2. Revised Length (LTDS & Rock)	Dry	1.45 (-7%)
3. End of Construction (Not LTDS, Only ID)	Dry	1.70

2D Stability Analyses

Design Cases			
Case	Name	Scenario	Notes
1	Initial Design – Rock	L1+G1+S1+Drained	Grid Long-Term Design Strength (LTDS=66.1 kN/m) & Uniform 175 ft
2	Revised Length - Rock	L2+G1+S1+Drained	Grid LTDS, variable grid length (80-175 ft), & 36^0
3	End of Construction (Short-Term)	L2+G2+S2+Drained	Exhumed grid strength (145.9 kN/m-ID), variable grid length, & 36^0
4	End of Construction (FSS)	L2+G2+S3+GW	FSS, exhumed grid strength (145.9 kN/m-ID), variable grid length, & GW
5	Failure (FSS)	L2+G3+S3+GW	FSS, exhumed grid strength (ID) + Creep (84.8 kN/m), variable grid length, & GW

2D Stability Results

Factors of Safety for Cases 4-5 with Groundwater			
Design Case	Water Condition	Geogrid Tensile Resistance Model	2D FS $FS_{2D} < 1.5$
4. End of Construction (FSS)	Dry	Isotropic	1.15
	Low	Isotropic	1.15
	Medium	Isotropic	1.13
	High	Isotropic	1.13
5. Failure	Dry	Isotropic	1.03
	Low	Isotropic	1.01
	Medium	Isotropic	0.99
	High	Isotropic	0.95

Outline

- 12 March 2015 Failure
- Laboratory Testing
- 2D Limit Equilibrium Analyses
- 3D Limit Equilibrium Analyses
- Continuum Deformation Analyses
- Summary

Uses of 3D Analyses in Practice

- **Overlap, anisotropy, different grids, & water**

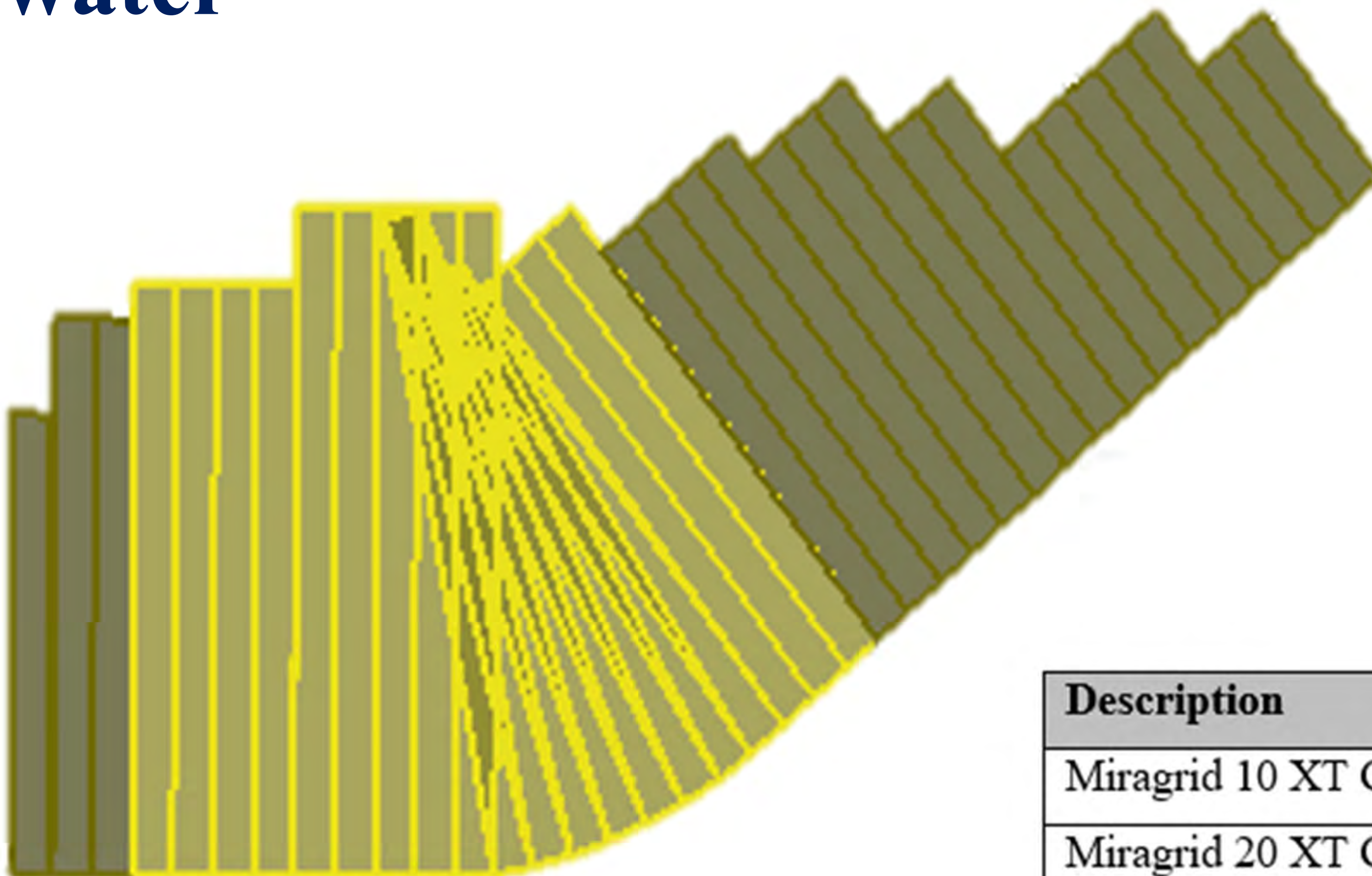

Description	Color
Miragrid 10 XT Geogrid	
Miragrid 20 XT Geogrid	

Stark et al. (2021) ©

2D v. 3D Slope Stability

- 2D analyses assume plane strain condition
- Slopes are not infinitely wide
- 3D effects influence stability

Stark et al. (2021) ©

2D v. 3D Slope Stability

BC Hydro

California DWR

REQUIRED 3D FACTOR OF SAFETY

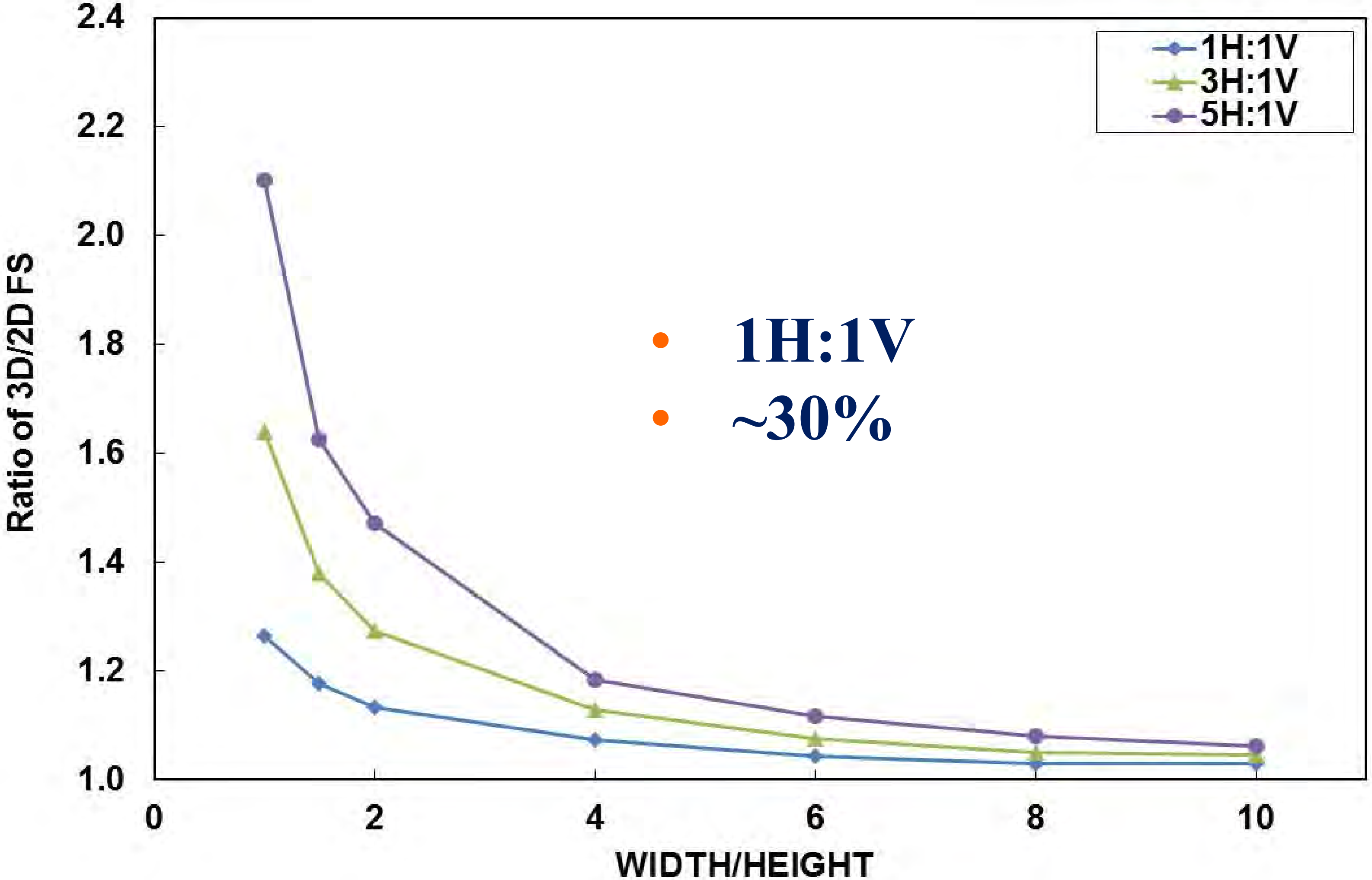

- 1H:1V
- ~30%

Akhtar and Stark (2017)

Quiz

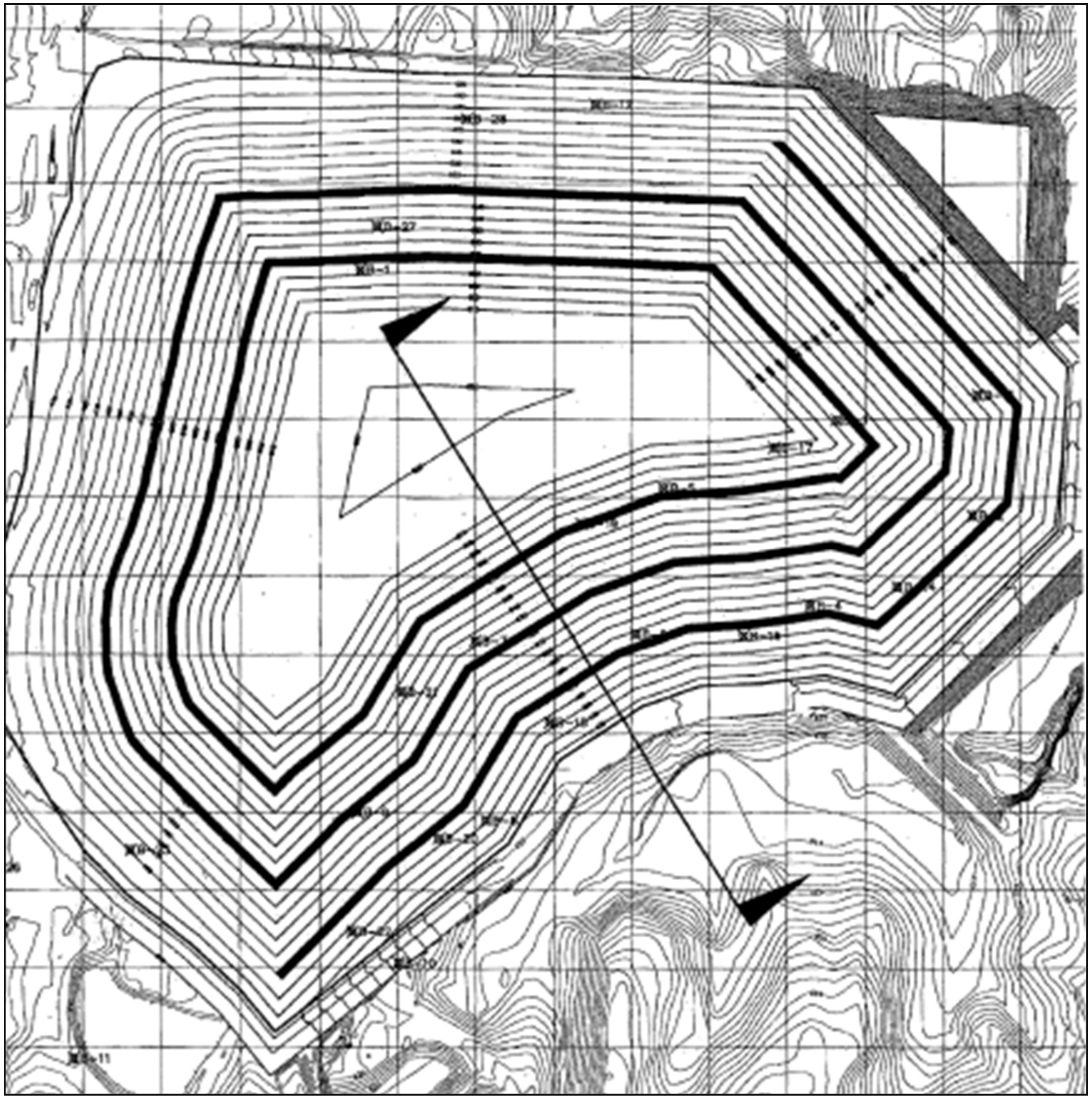

Stark et al. (2021) ©

Yeager Airport 3D Effects

Stark et al. (2021) ©

- **Uni-Axial Geogrid**

Stark et al. (2021) ©

- **90% reduction b/t MD and XMD**

Exhumed Geogrid Testing Results

Exhumed MD Geogrid Wide Width and Single Rib Tests				Testing XMD Geogrid
Geogrid Type	Wide Width strength (lbs/ft)	Single Rib Strength (lbs/ft)	Strength Used in Analysis (lbs/ft)	Strength Used in Analysis (lbs/ft)
A	7,511	9,165	9,000	900 (-90% at 60^0)
B	9,037	9,848	10,000	1,000

Uses of 3D Analyses in Practice

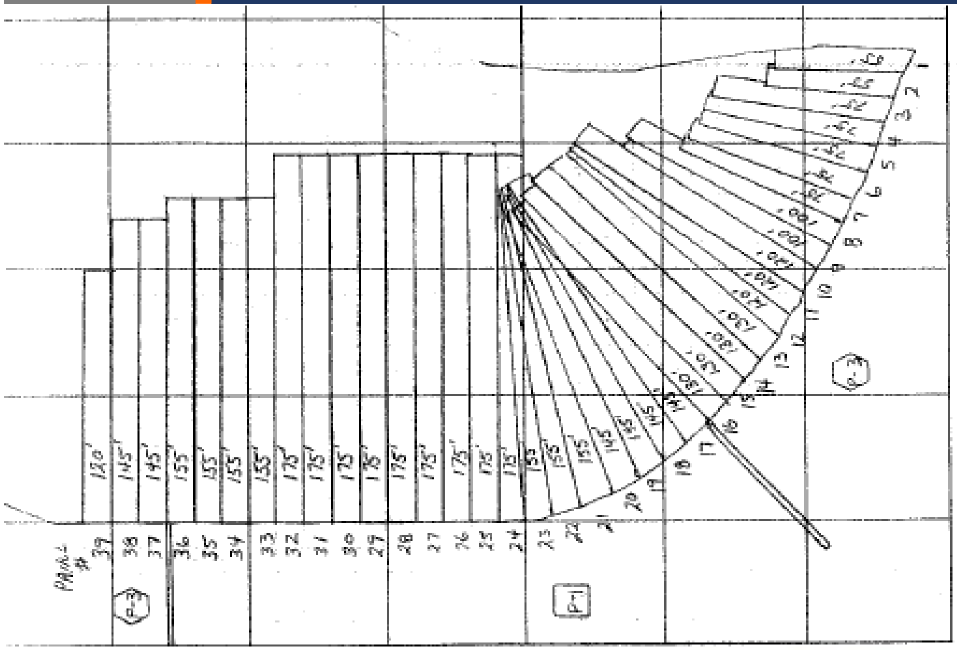

- El. +875 ft
- 85 layers of geogrid
- Method A – T horizontal at slice base
- $\geq 60^0$ = XMD

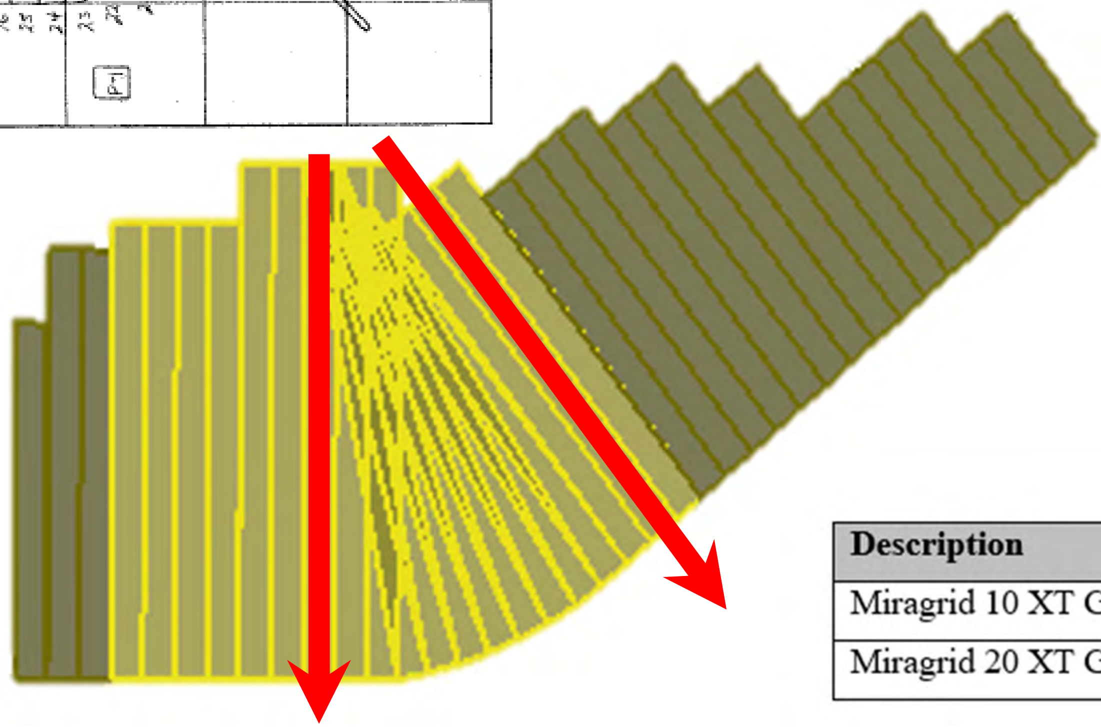

Description	Color
Miragrid 10 XT Geogrid	
Miragrid 20 XT Geogrid	

FGI Fabricated Geomembrane Institute

Geogrid Layers

- **All 3 ft**

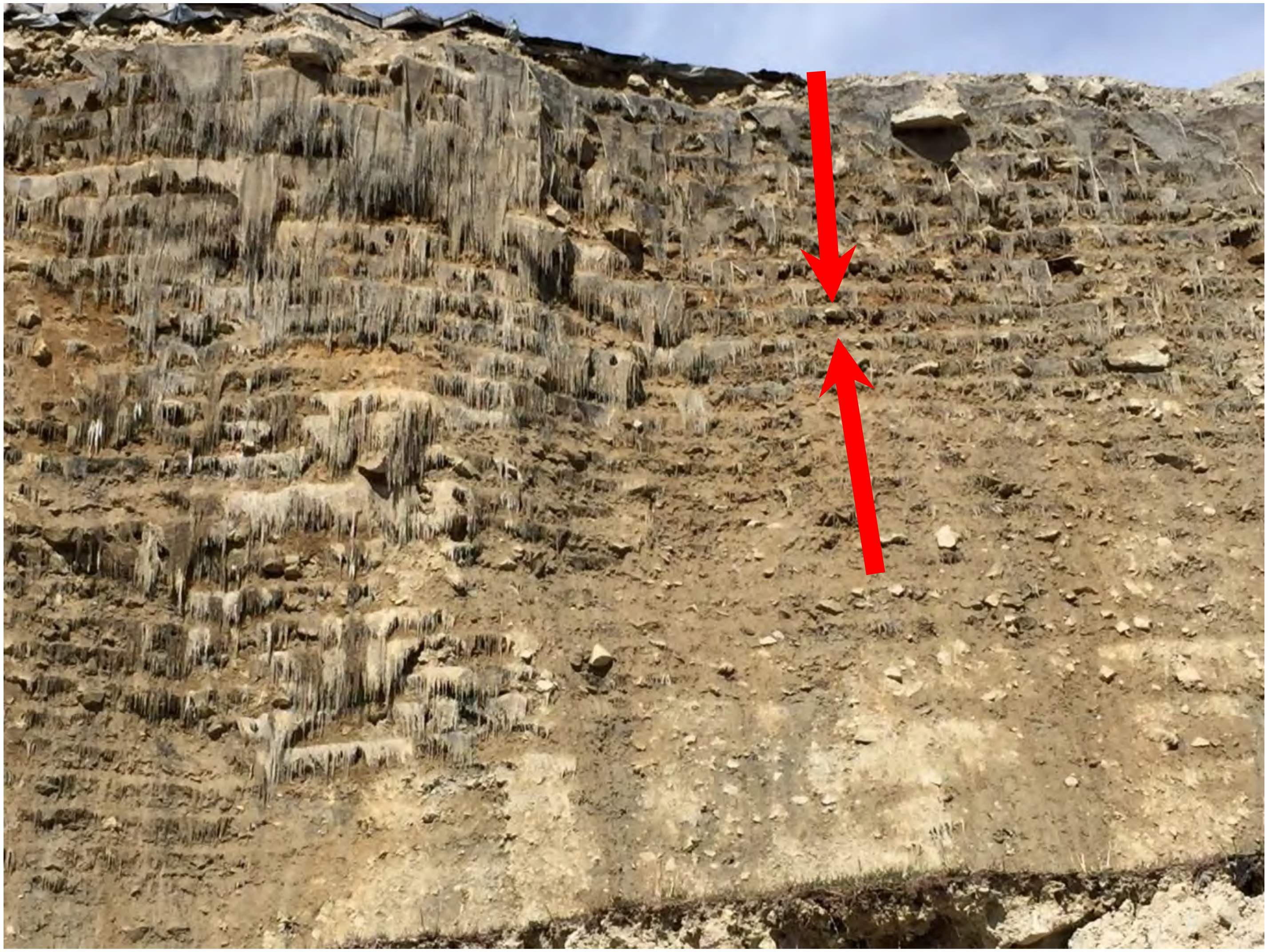

- **El. 710.0 to 744.5 ft = every 1.5 ft vertically**
- **Above El. 746.0 ft = every 3.0 ft vertically**

3D Analysis of Geogrids

- 90% reduction b/t MD and XMD

3D Analyses

- **3D Geometry, Slide Mass, Anisotropy, & High GW**

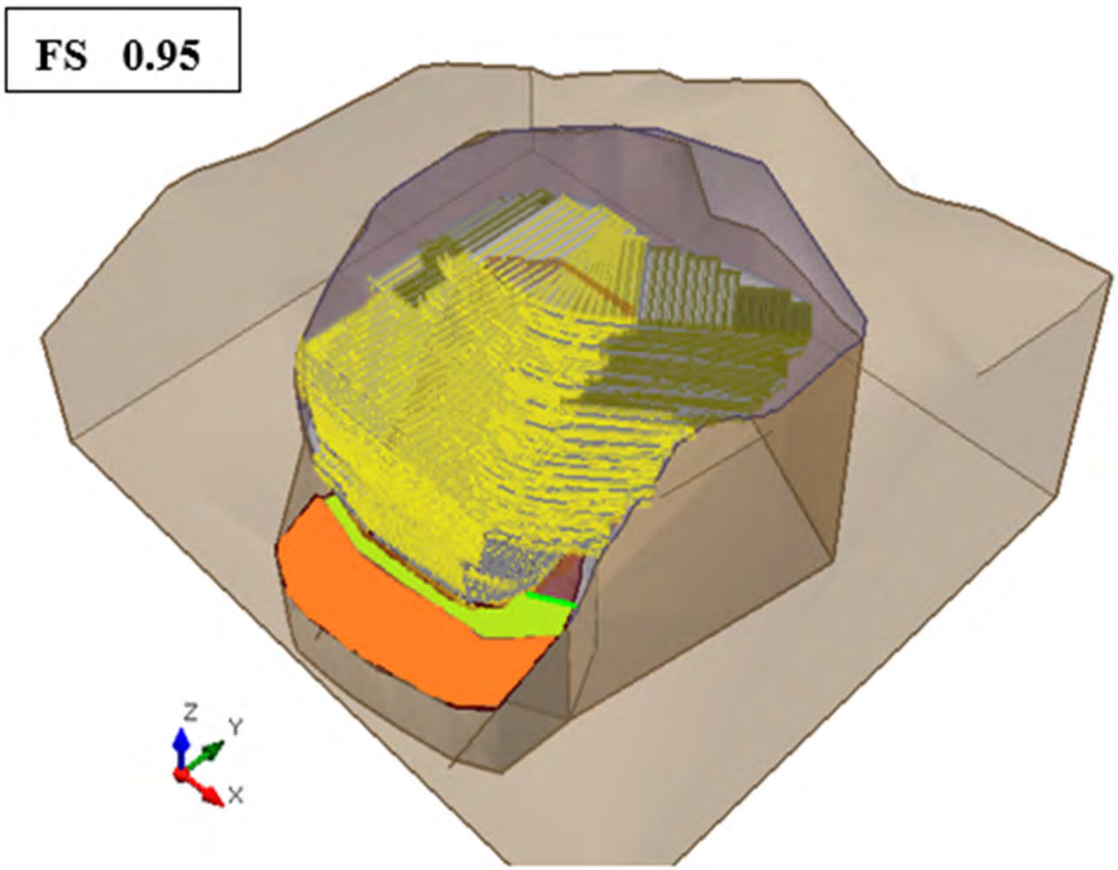

Legend

Description	Color
Reinforced Soil	
In-Situ Soil	
Bearing Soil	
Soil-Rock Interface Zone	
Rock	
Miragrid 10 XT Geogrid	
Miragrid 20 XT Geogrid	

3D Stability Results

Design Scenarios	Geogrid Tensile Resistance Model	3D FS	2D FS
$FS_{(1: \text{Initial Design})}$	Isotropic	1.65	1.54 -8%
	Anisotropic	1.52	
$FS_{(2: \text{Revised Design})}$	Isotropic	1.51	1.45
	Anisotropic	1.44	
$FS_{(3: \text{End of Construction: Peak})}$	Isotropic	1.95	1.70
	Anisotropic	1.75	

- **0.13 or ~8% decrease**
- **All cases 5 to 15% decrease for anisotropy**

Uses of 3D Analyses in Practice

- **Decrease in FS with Time**

Design Scenarios	Geogrid Tensile Resistance Model	Groundwater (GW)			
		Dry	Low	Medium	High
FS (4: End of Construction: FSS)	Isotropic	1.43	1.42	1.37	1.27
	Anisotropic	1.27	1.26	1.21	1.13
FS(5: Failure)	Isotropic	1.15	1.14	1.09	1.02
	Anisotropic	1.08	1.07	1.03	0.95

- **Failure w/isotropic grids & high GW or**
- **Failure w/anisotropic grids & medium GW**

Summary 3D Stability Analyses

Case	Design Case	2D FS with Isotropic Tensile Force	3D FS with Anisotropic Tensile Force
1	Initial Design	1.54	1.52
2	Revised Design	1.45	1.44
3	End of Construction (Peak) - Dry	1.70	1.75
4	End of Construction (FSS) - Medium	1.13	1.21
5	Failure - Medium	0.99	1.03

- **2D ~ 3D**
- **3D NOT 10 - 30% higher**
- **2D not conservative w/uniaxial grids**

3D Stability Analysis Summary

- Not accounting for anisotropic tensile resistance decreases 3D FS ~ 5 to 15%
- 2D stability analyses not conservative with anisotropic reinforcement
- Failure occurred with anisotropic grids and medium GW
- 3D FS ~ 1.9 to match 2D FS ~ 1.5

Foundation Failure Outline

- 12 March 2015 Failure
- Laboratory Testing
- 2D Limit Equilibrium Analyses
- 3D Limit Equilibrium Analyses
- Continuum Deformation Analyses
- Summary

FLAC3D Model – 2D cross-section T-T - Domain

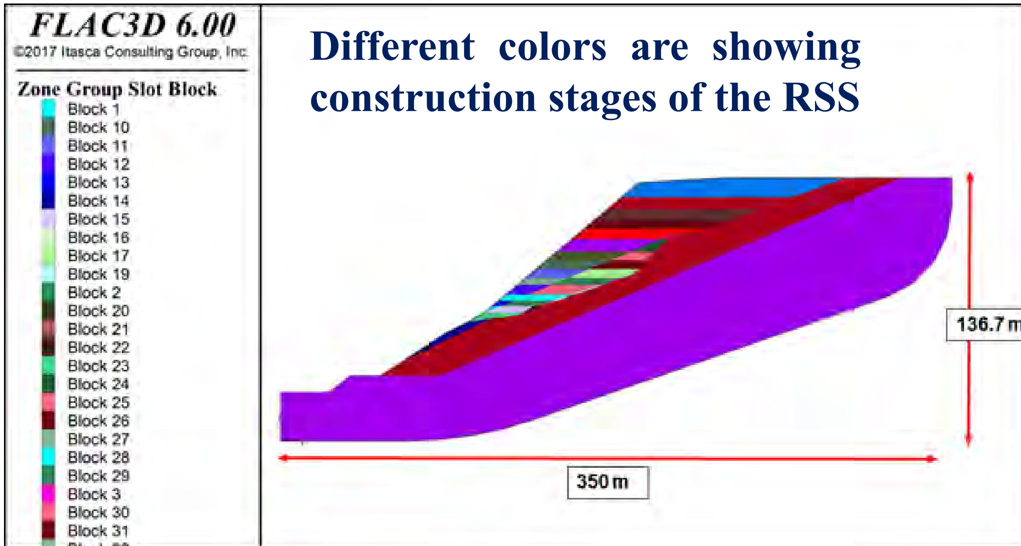

The domain is 350x137 m (1167x457 ft).
The thickness of the model is 0.25 m. The shear zone was modeled explicitly with zones while the RSS-Rock contact with an interface.

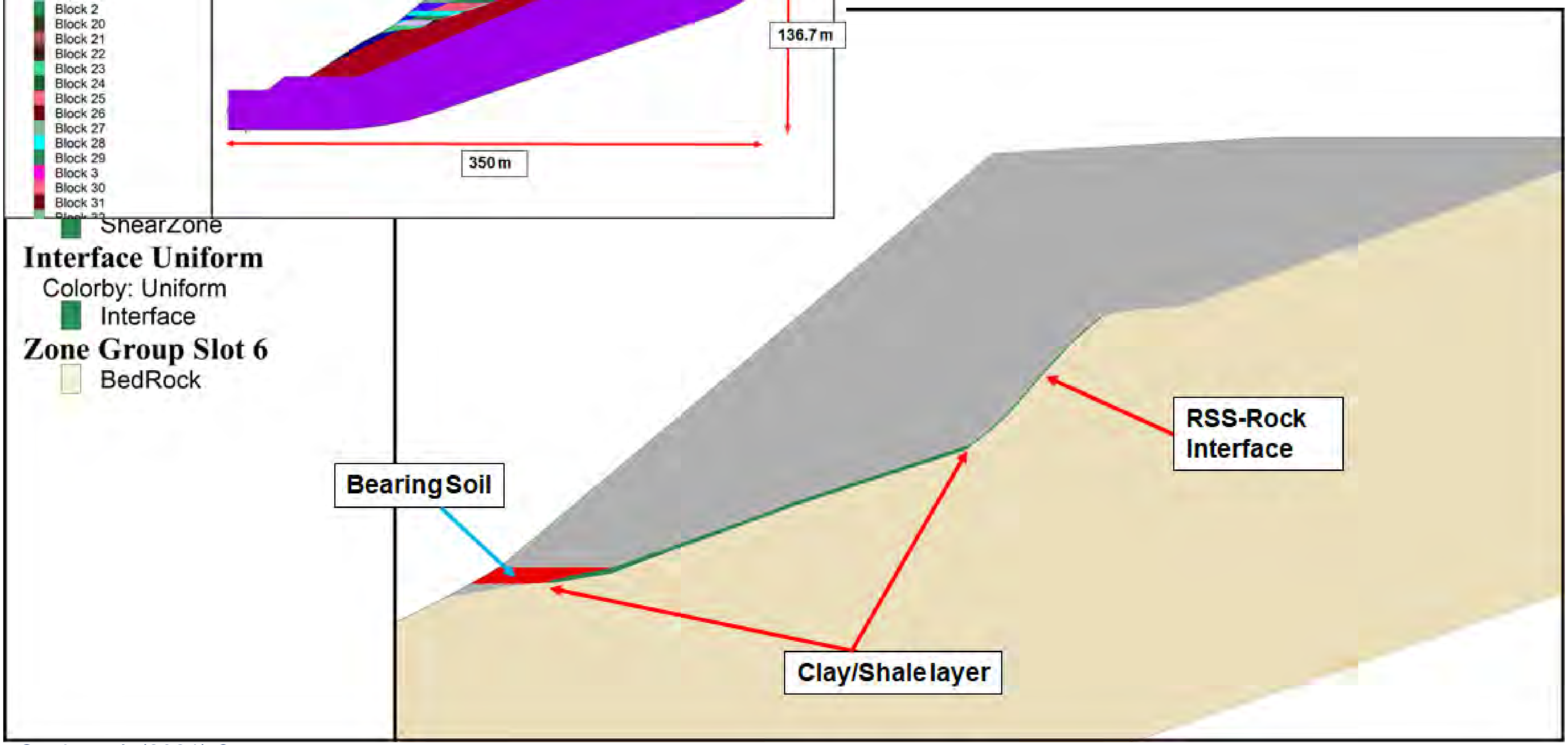

FLAC3D Model – 2D cross-section T-T - Domain

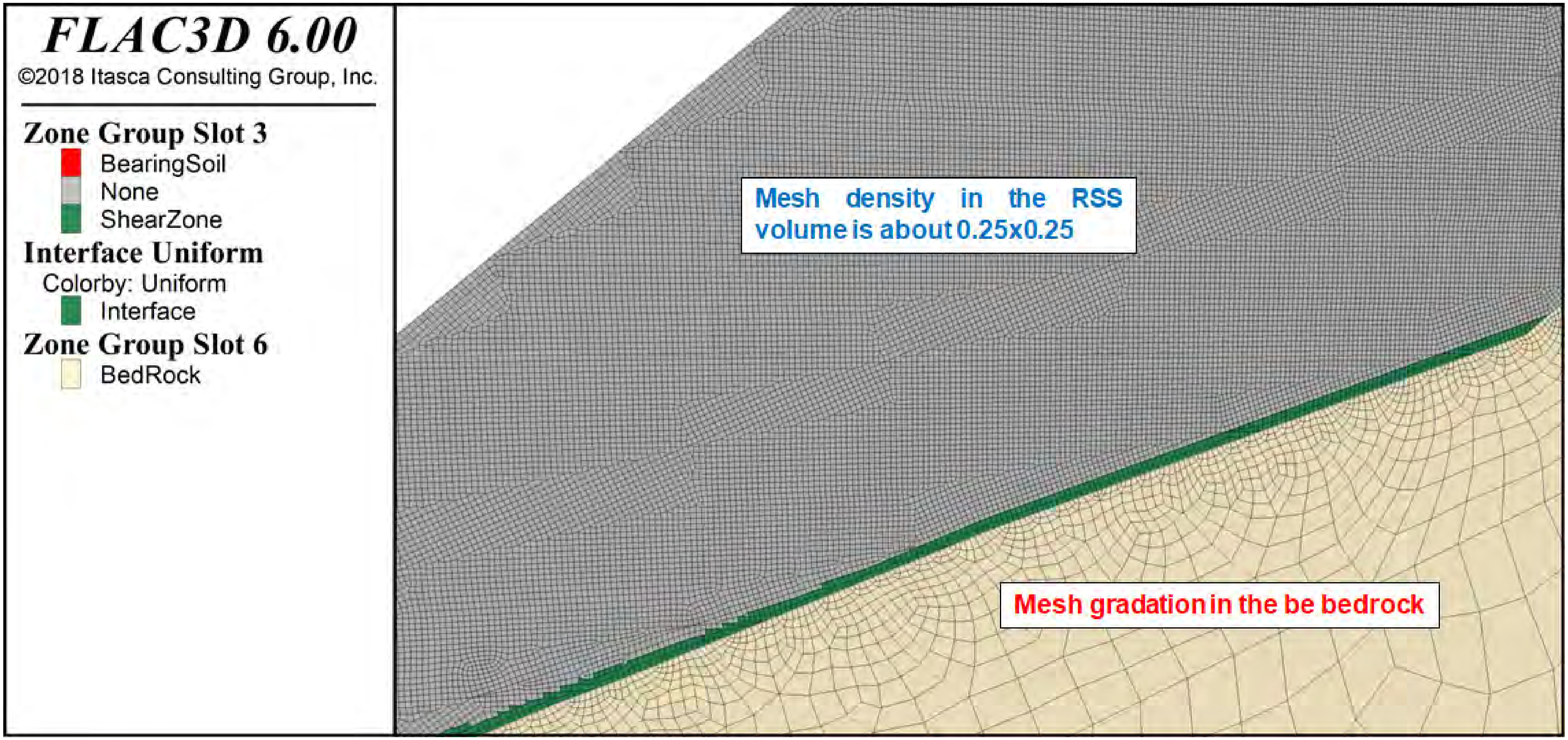

RSS and Shear zone mesh detail. The mesh was created importing a DXF file inside the extruder. The model has 75291 quad-dominant zones and 151254 gridpoints. It is a small model because of the numerous runs expected to test different hypothesis.

FLAC3D Model – RSS stiffness scenario for SRM

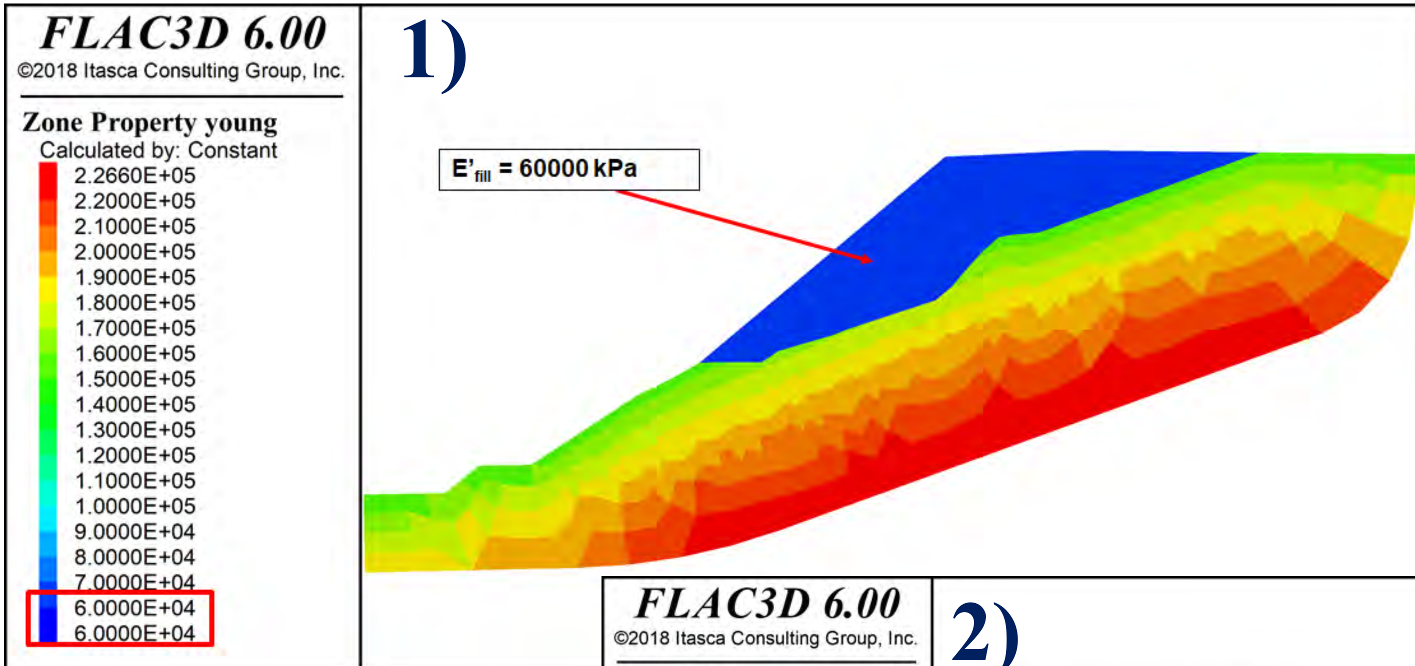

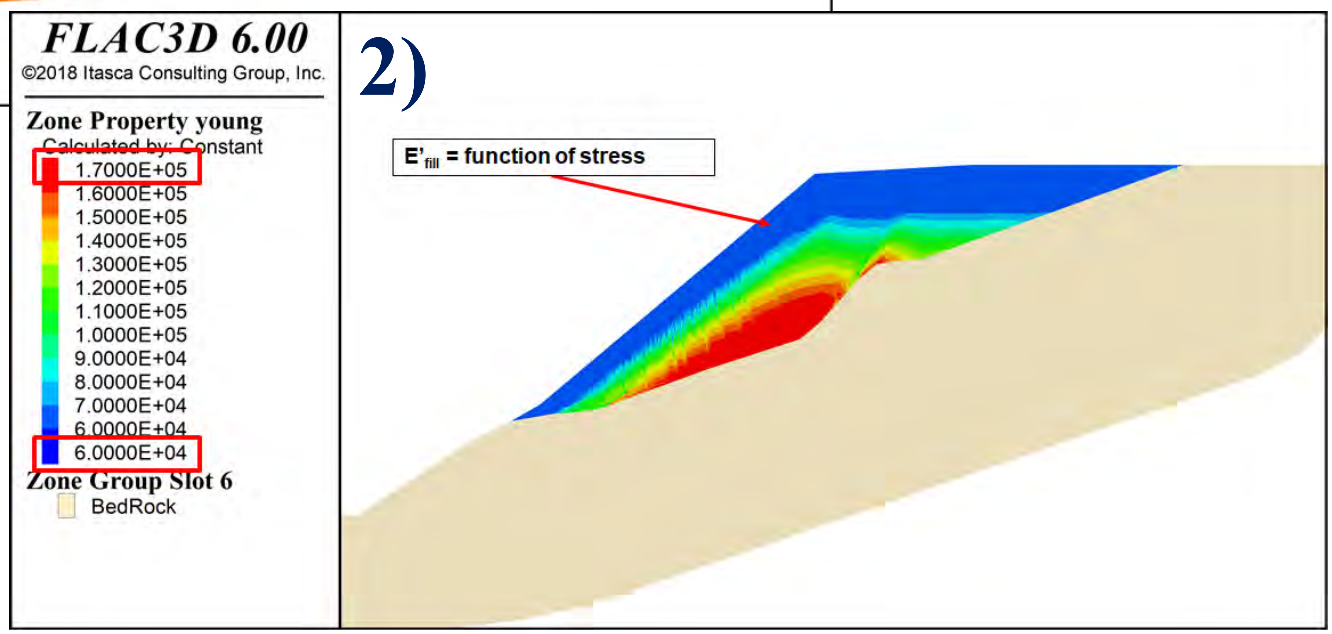

The reason for considering a stress dependent modulus inside the fill is to investigate the potential effect on the stress mobilization pattern in the reinforcement during the strength reduction process leading to significantly different internal (inside the fill mass) shear band formation.

FLAC3D Model – Reinforcement

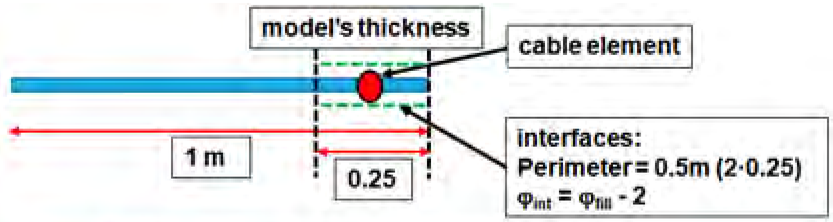

TDS_MG20XT | deformation @ failure = 8%

Mechanical Properties	Test Method	Unit	Machine Direction Value
Tensile Strength @ Ultimate (MARV[1])	ASTM D6637 (Method B)	lbs/ft (kN/m)	13705 (200.0)
Tensile Strength @ 5% strain (MARV[1])	ASTM D6637 (Method B)	lbs/ft (kN/m)	5340 (77.9)
Creep Rupture Strength[2]	ASTM D5262/D6992	lbs/ft (kN/m)	9452 (137.9)
Long Term Design Strength[3]		lbs/ft (kN/m)	7540 (110.0)

EA = 200/0.08*0.25 = 625 kN

Manufactured properties:

Fy_t0 = 200*0.25 = 50 kN/0.25m

EA_t0 = 625 kN/0.25m

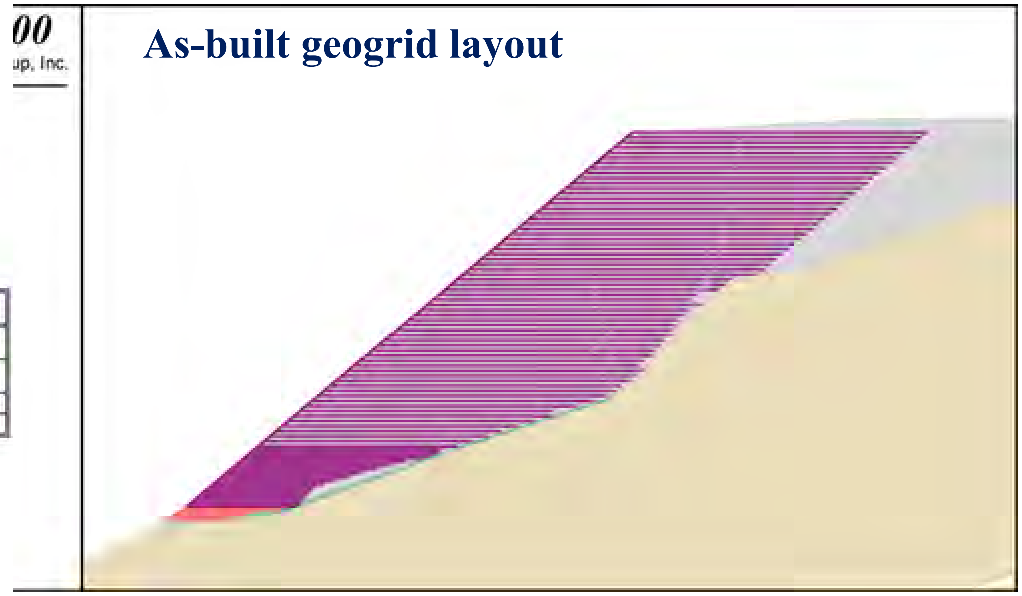

The geogrid has been modeled using cable elements. These elements allow for setting a limit tensile strength; if the tensile strength is reached somewhere during the analysis, the failed element is deleted from the model. The initial ultimate force in the MD is considered during the construction of the RSS. At the end of the construction sequence, before starting the strength reduction process in the shear zone, the geogrid mechanical properties are modified according to the exhumed strength and stiffness measured during the forensic tests, as shown in the following figures.

Stark et al. (2021) ©

FLAC3D Model – Stage 2 – Geogrid mobilization

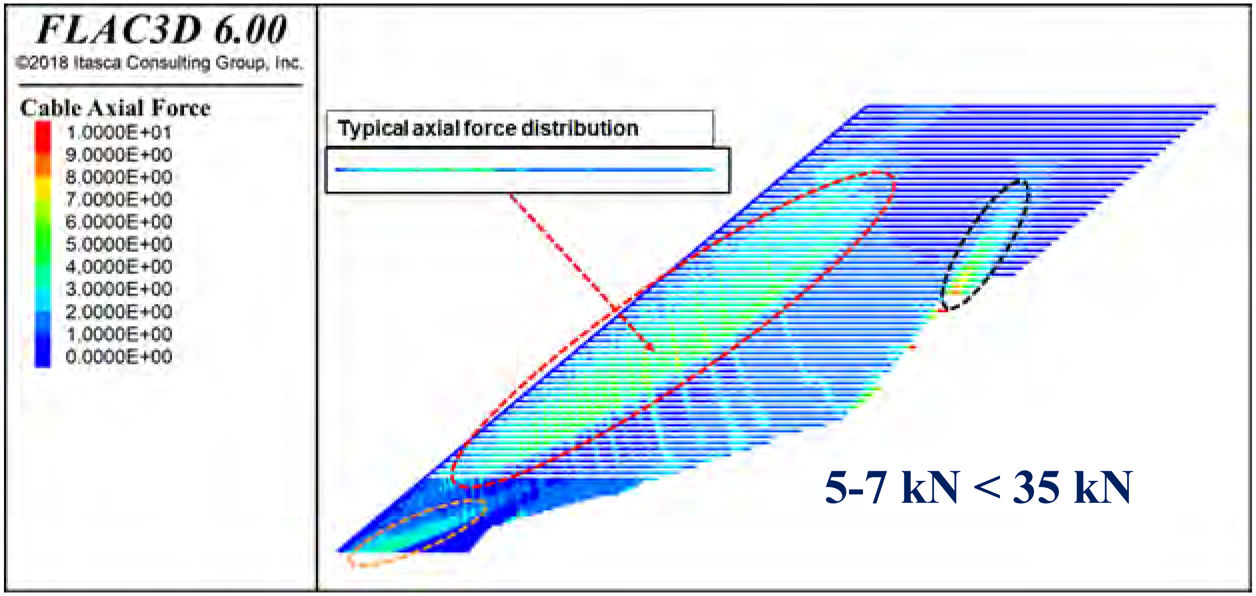

Axial Force and strain distribution in the geogrids.

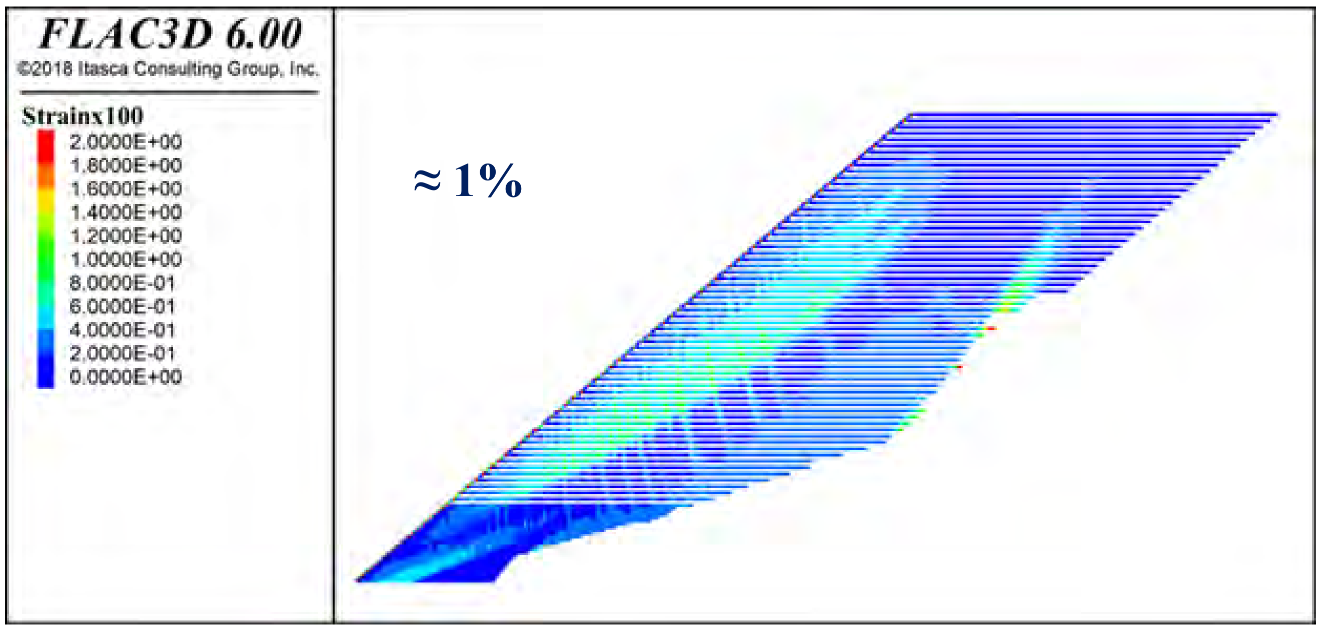

FLAC3D Model – Stage 3a – Exhumed prop, PP=Medium

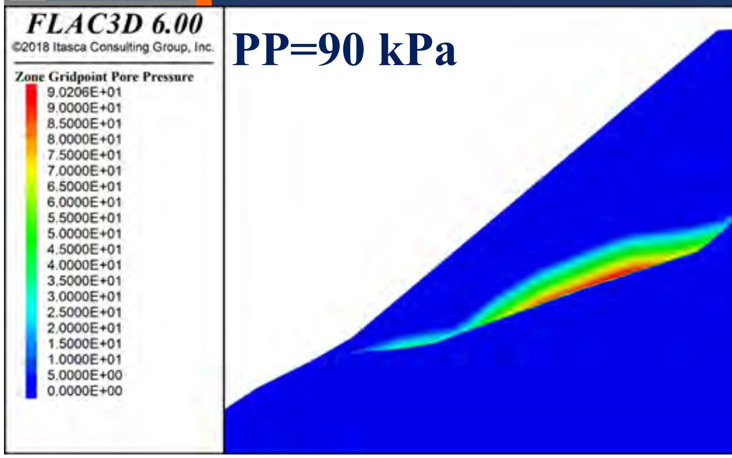

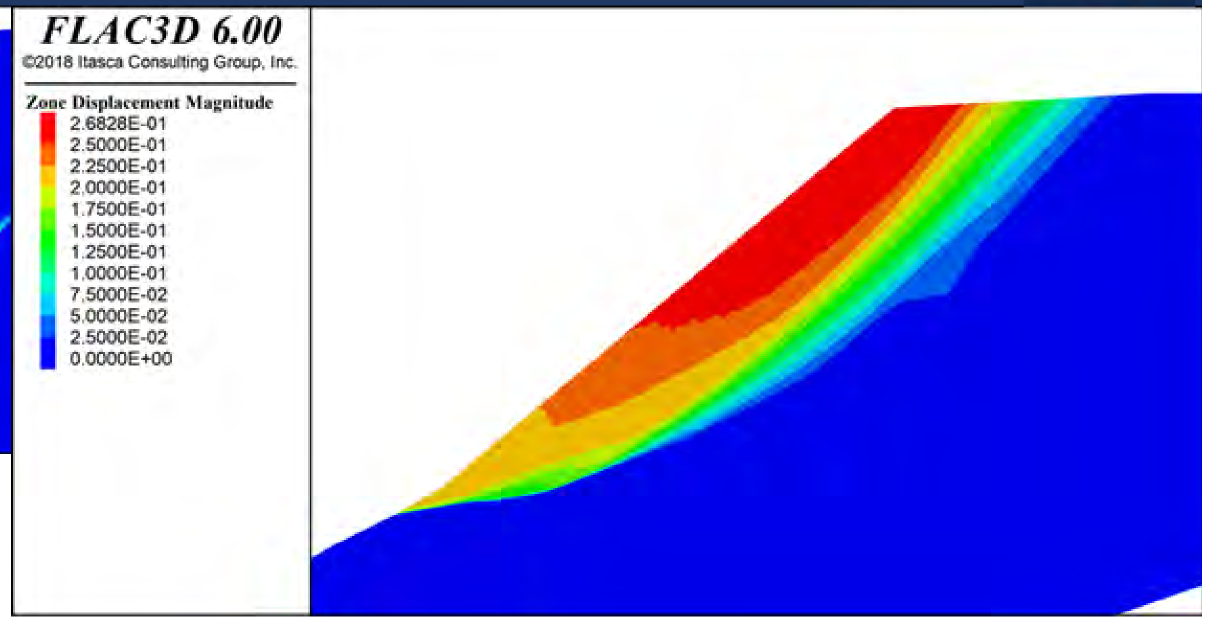

Now we see a significant increment in displacement and a much larger mobilization of the effort in the geogrid.

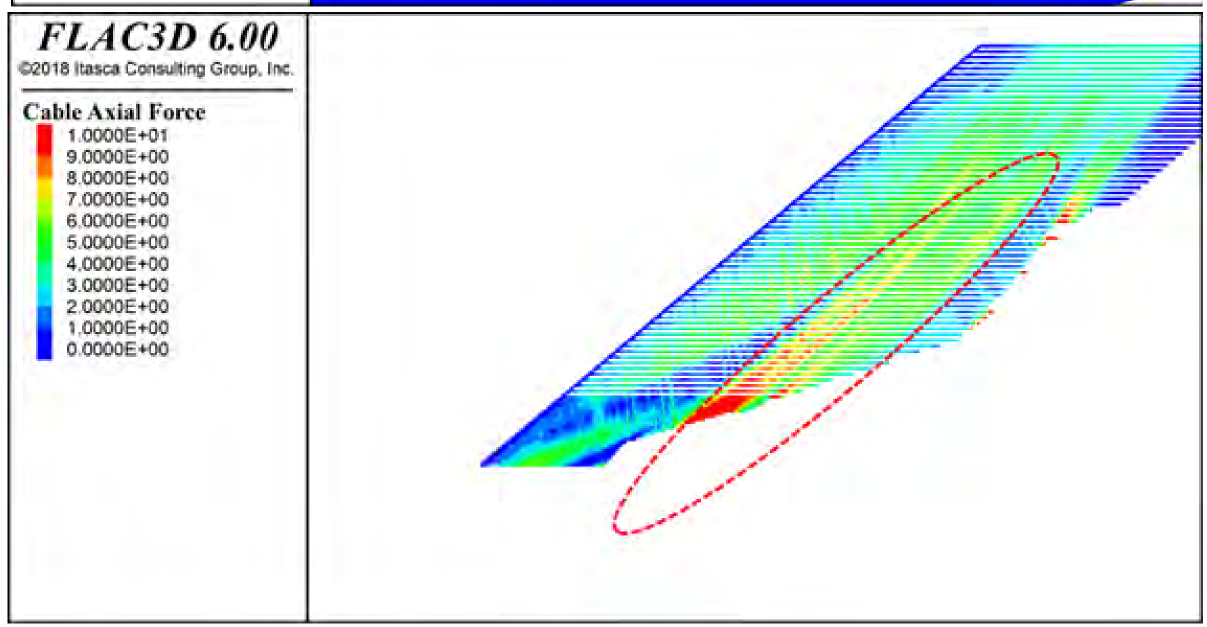

FLAC3D Model – Stage 3a – Exhumed prop, PP=Medium

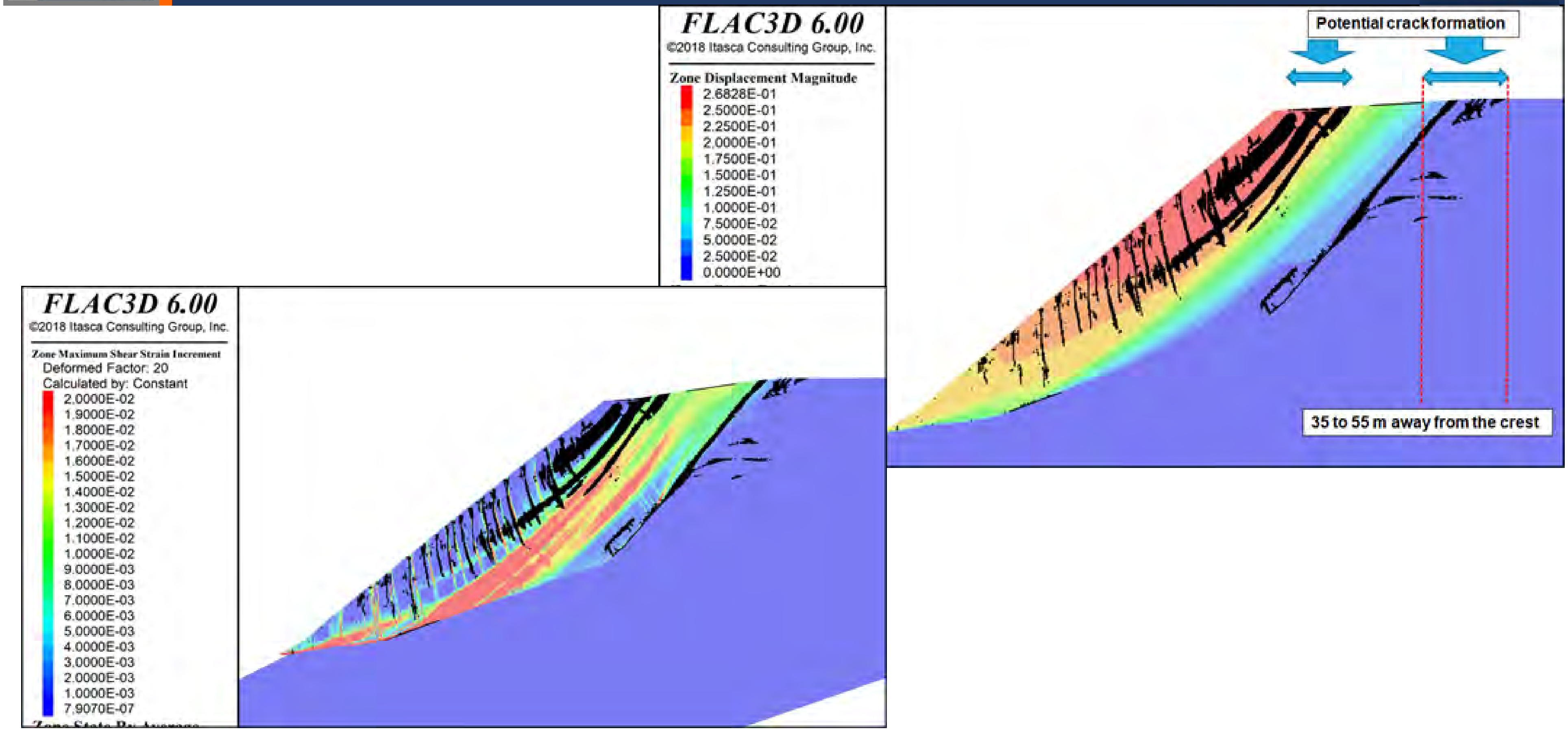

The figure show the shear band location inside the RSS fill overlapped with the incremental displacement field and the shear strains. There is a significant volume of the RSS fill that is already over 2% of shear strain potentially leading to crack formation at the ground surface. The most likely region for crack formation is expected around 35 to 55 m away from the crest in correspondence of section T-T.

FLAC3D Model – Shear zone strength reduction

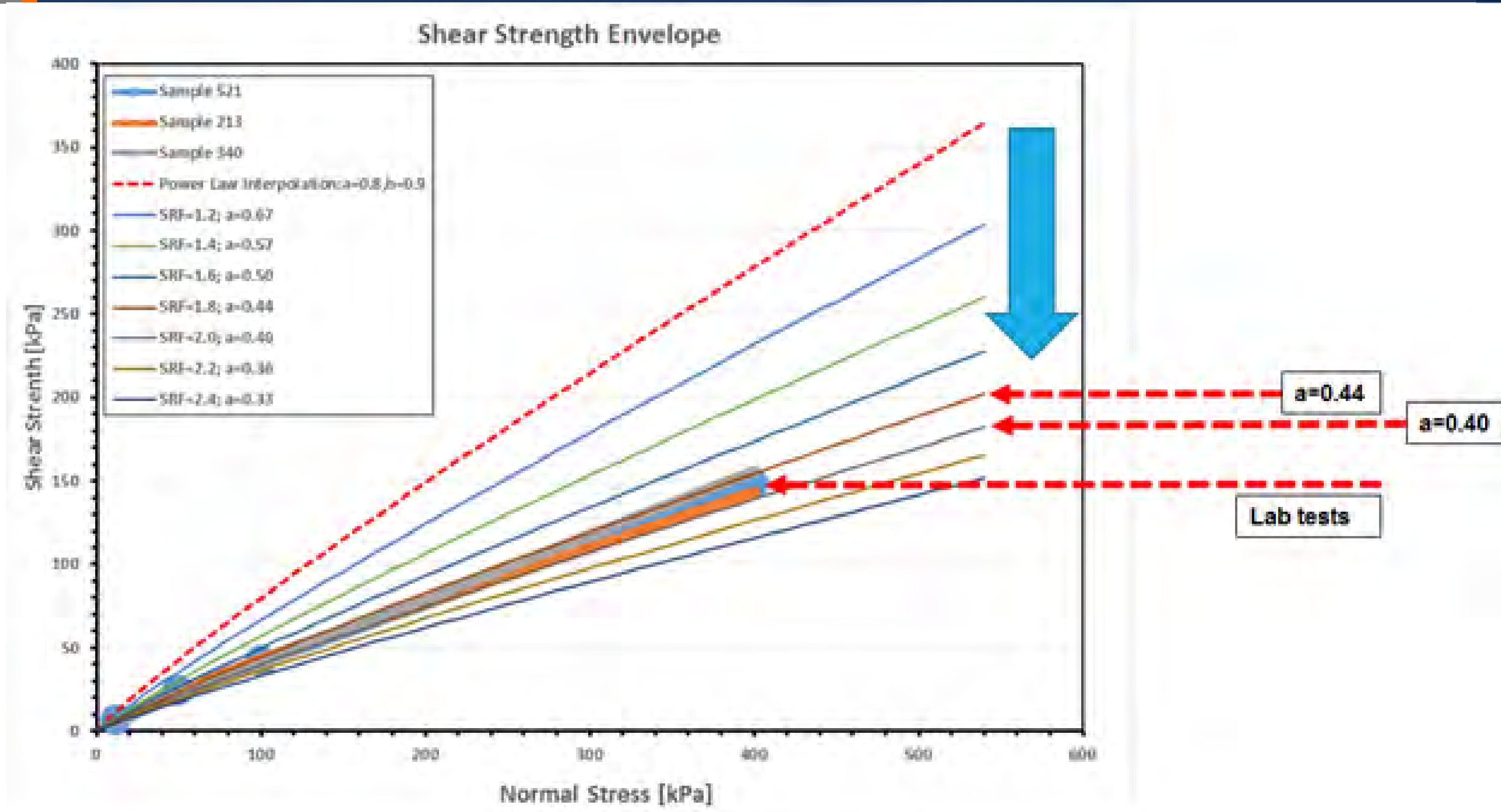

The shear zone strength is reduced gradually applying an incremental reduction factor of 0.01 to the paraments a on each step of the process. Initially the SRF is equal to 1 than is incremented in step of 0.01 so that step two has a SRF of 1.01 and so on until failure is detected.

Stark et al. (2021) ©

FLAC3D Model – Results – Stage 4-1c – PP=Medium

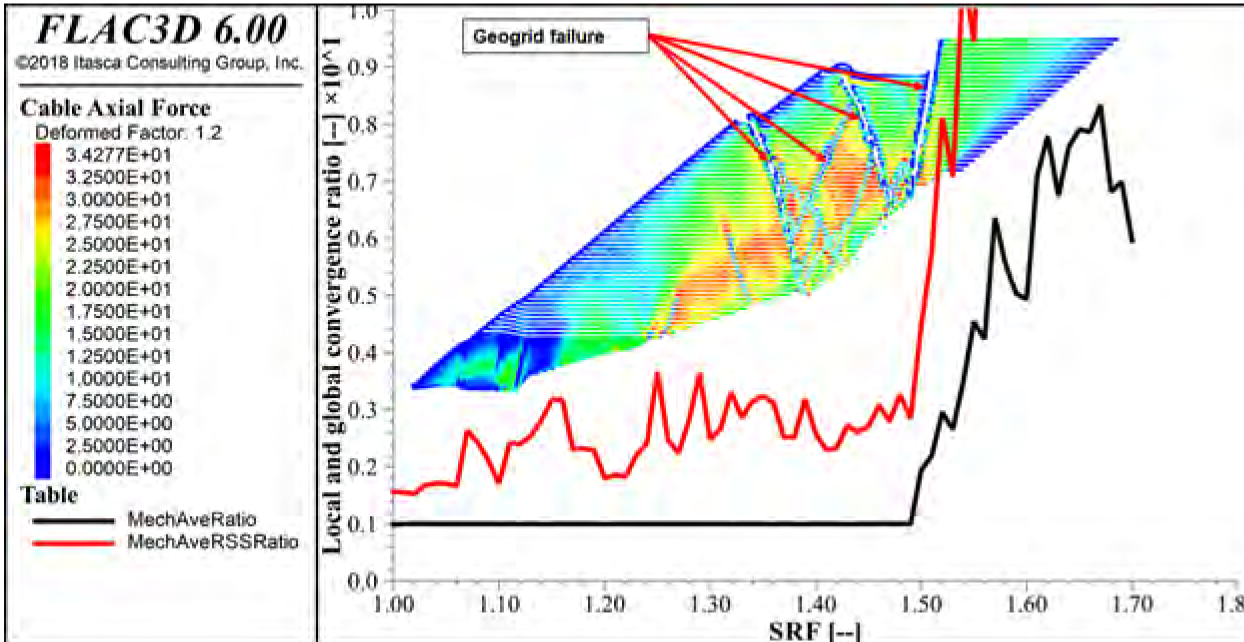

The model converges up to SRF = 1.460 and becomes clearly unstable after. The corresponding *a* parameter of the strength envelope is therefore:

$$a_{min} = a_{ini}/SRF_{st} = 0.800/1.460 = 0.537$$

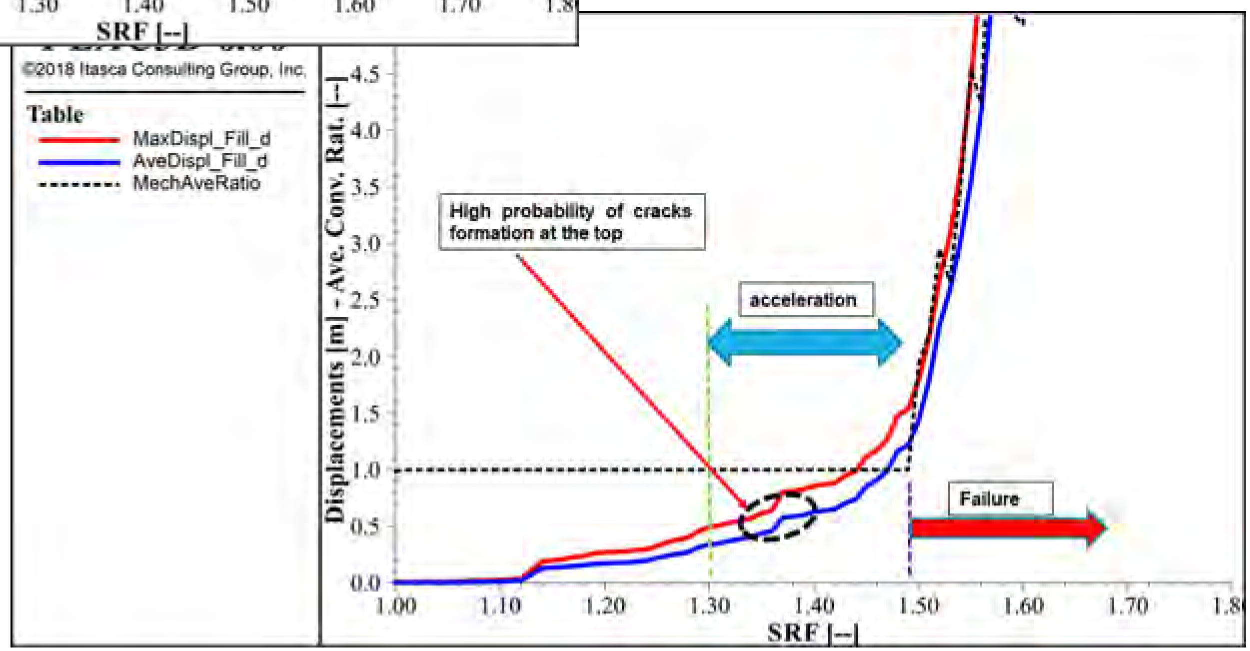

Stark et al. (2021) ©

FLAC3D Model – Summary

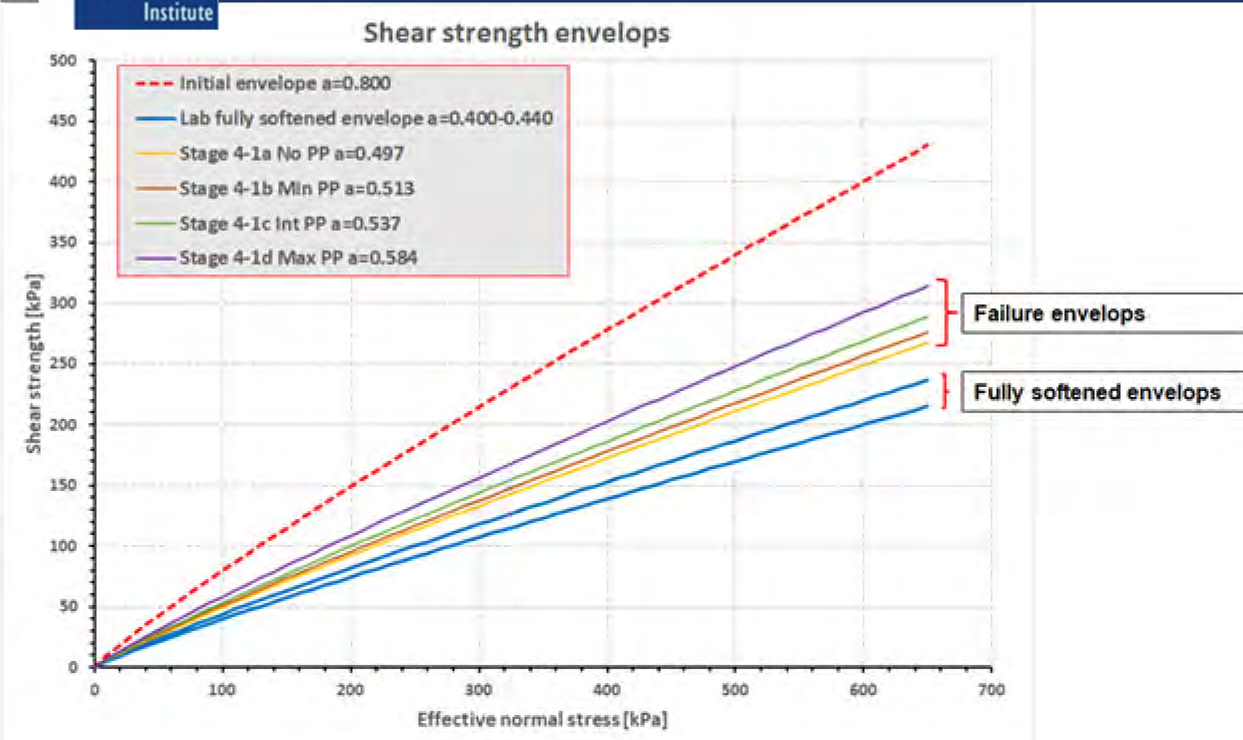

Stage	Pore Pressure	SRF	a
4-1a	No	1.610	0.497
4-1b	Minimum	1.560	0.513
4-1c	Intermediate	1.490	0.537
4-1d	Maximum	1.370	0.584
4-2a	No	1.600	0.500
4-2d	Maximum	1.390	0.576

It is expected to observe lower shear strength from fully remolded samples after a large failure that has determine a significant amount of shearing in the material. Moreover, the analyses presented here are in 2-dimensional conditions while the mechanism in the field is clearly 3-dimensional.

Fully softened a = 0.42. **$0.42 \cdot 1.3 = 0.55$**

FLAC3D Model – Example Movie – Stage 4-1d PP=Mediu

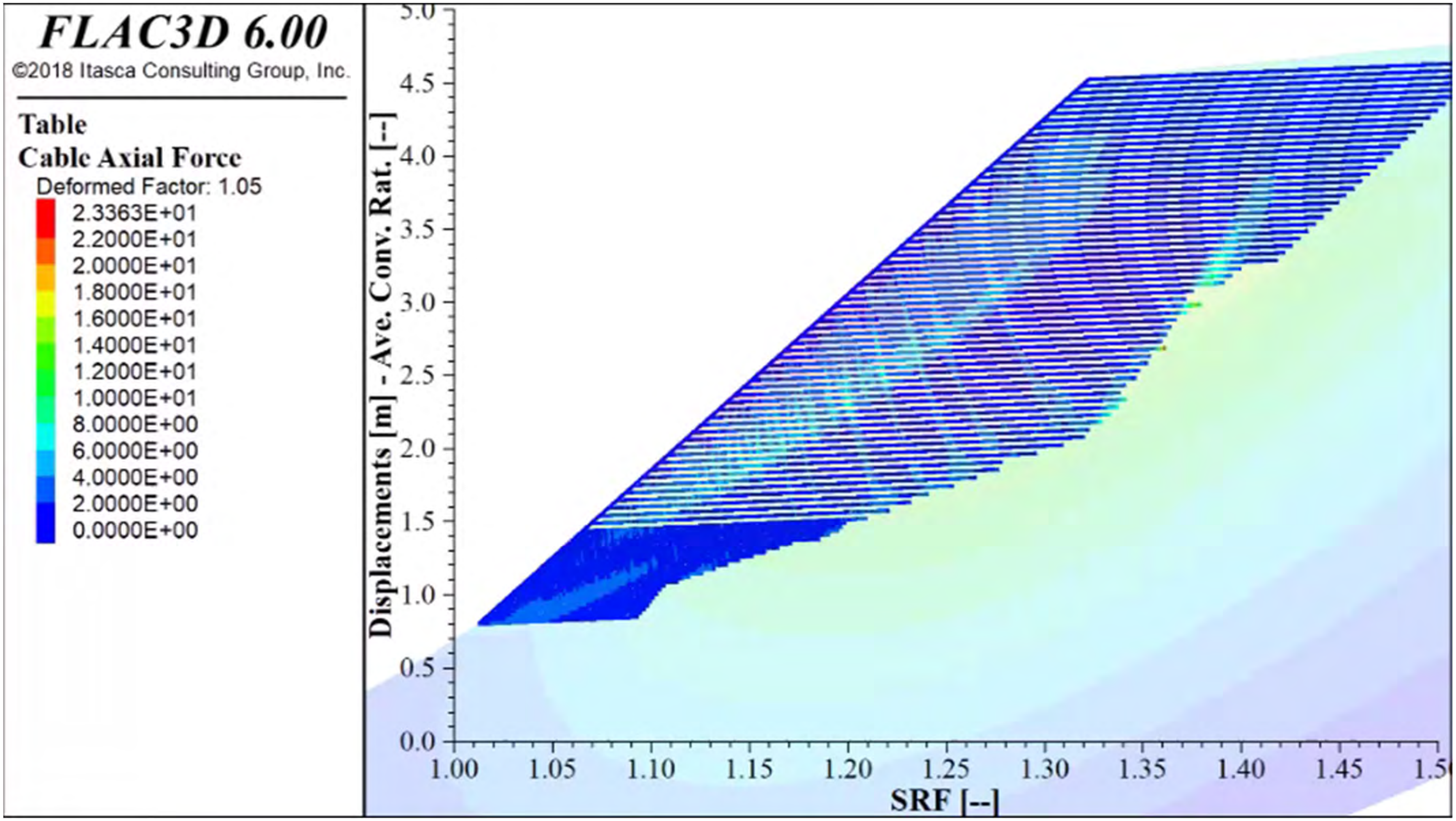

Fundao Failure Outline

- 12 March 2015 Failure
- Laboratory Testing
- 2D Limit Equilibrium Analyses
- 3D Limit Equilibrium Analyses
- Continuum Deformation Analyses
- Summary

Causation Summary

- Failure caused by:
  - shortened geogrids in lower slope
  - bearing soil at toe
  - reduction in soil strength from peak value
  - anisotropic tensile resistance
  - reduction in tensile strength due to construction and creep
  - increased GW from dry to medium

Contact Information

Jim Collin, Ph.D., P.E., D.GE., F. ASCE
President
The Collin Group, Ltd.
jim@thecollingroup.com

Augusto Lucarelli, P.E.
Principal Engineer
Itasca Consulting Group
alucarelli@itascacg.com

Timothy D. Stark Ph.D., P.E., D.GE., F. ASCE
Professor of Civil & Environmental Engineering
University of Illinois at Urbana-Champaign
Technical Director
Fabricated Geomembrane Institute
tstark@Illinois.edu

Jennifer Miller, M.S.
Coordinator
Fabricated Geomembrane Institute
University of Illinois at Urbana-Champaign
fabricatedgeomembrane@gmail.com

Next FGI Webinar

Geomembrane Attachment and Penetration Design and Installation

Thursday, February 4, 2021 at 11 am CST

Free to Industry Professionals

1.0 PDH

Presenter

Patrick Elliott – Raven Industries/CLI

Brendan Simbeck and Duff Simbeck – Simbeck and Associates

Check out the FGI's Website

- Online PDH Program
- New!! Audio and Video Podcasts
- Latest Specifications and Guidelines
- Installation Detail Drawings (PDF and DWG)
- Technical Papers and Journal Articles
- Webinar Library (available to view and download video & related materials)
- ASTM Field and Laboratory Test Method Videos
- Pond Leakage Calculator
- Panel Weight Calculator
- Photo Gallery
- Member Directory
- Material and Equipment Guides
- Industry Events Calendar
- Women in Geosynthetics

www.fabricatedgeomembrane.com